Science of the Total Environment 851 (2022) 158062

Contents lists available at ScienceDirect

Science of the Total Environment

journal homepage: www.elsevier.com/locate/scitotenv

New tree-ring data from Canadian boreal and hemi-boreal forests provide insight for improving the climate sensitivity of terrestrial biosphere models

A. Mirabel [a,b,*], M.P. Girardin [b], J. Metsaranta [c], E.M. Campbell [d], A. Arsenault [e], P.B. Reich [f,g,h], D. Way [a,i,j]

[a] Department of Biology, University of Western Ontario, London, Ontario, Canada
[b] Natural Resources Canada, Canadian Forest Service, Laurentian Forestry Centre, Quebec City, QC, Canada
[c] Natural Resources Canada, Canadian Forest Service, Northern Forestry Centre, Edmonton, AB, Canada
[d] Natural Resources Canada, Canadian Forest Service, Pacific Forestry Centre, Victoria, BC, Canada
[e] Natural Resources Canada, Canadian Forest Service, Atlantic Forestry Centre, Corner Brook, NL, Canada
[f] Department of Forest Resources, University of Minnesota, St. Paul, MN 55108, USA
[g] Hawkesbury Institute for the Environment, Western Sydney University, Penrith, NSW 2753, Australia
[h] Institute for Global Change Biology, School for the Environment and Sustainability, University of Michigan, Ann Arbor, MI 48109, United States
[i] Nicholas School of the Environment, Duke University, Durham, NC, USA
[j] Environmental & Climate Sciences Department, Brookhaven National Laboratory, Upton, NY, USA

HIGHLIGHTS

- Canadian boreal/hemi-boreal forests display a gradient in growth sensitivity to climate variability
- Terrestrial Biosphere Models (TBMs) reproduced the same growth limitation gradient observed in tree rings
- However, a strong mismatch was observed in the key seasonal climate variables underlying this gradient
- TBMs overestimated the positive effect of temperature on growth, and underestimated the detrimental effect of drought
- Improvement for TBMs could involve leaf conductance and rooting and carbohydrate reserve dynamics

GRAPHICAL ABSTRACT

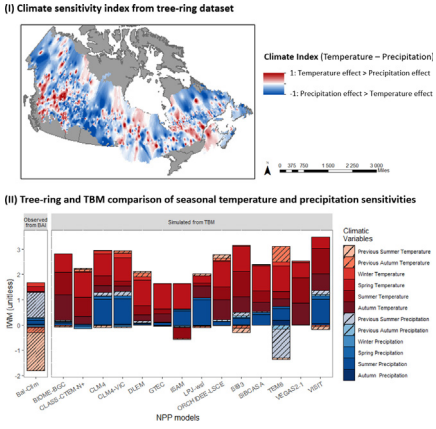

ARTICLE INFO

Editor: Elena Paoletti

Keywords:
Boreal/hemi-boreal forests
Dendroclimatology
Drought
Multi-scale Synthesis and Terrestrial Model Intercomparison Project (MsTMIP)
Forest productivity

ABSTRACT

Understanding boreal/hemi-boreal forest growth sensitivity to seasonal variations in temperature and water availability provides important basis for projecting the potential impacts of climate change on the productivity of these ecosystems. Our best available information currently comes from a limited number of field experiments and terrestrial biosphere model (TBM) simulations of varying predictive accuracy. Here, we assessed the sensitivity of annual boreal/hemi-boreal forest growth in Canada to yearly fluctuations in seasonal climate variables using a large tree-ring dataset and compared this to the climate sensitivity of annual net primary productivity (NPP) estimates obtained from fourteen TBMs. We found that boreal/hemi-boreal forest growth sensitivity to fluctuations in seasonal temperature and precipitation variables changed along a southwestern to northeastern gradient, with growth limited almost entirely by temperature in the northeast and west and by water availability in the southwest. We also found a lag in growth climate sensitivity, with growth largely determined by the climate during the summer prior to ring formation. Analyses of NPP sensitivity to the same climate variables produced a similar southwest to northeast gradient in growth

* Corresponding author at: Centre de foresterie des Laurentides, 1055 Rue du Peps, Québec, QC G1V 4C7, Canada.
E-mail address: ariane.mirabel@gmail.com (A. Mirabel).

http://dx.doi.org/10.1016/j.scitotenv.2022.158062
Received 8 April 2022; Received in revised form 28 July 2022; Accepted 12 August 2022
Available online 15 August 2022

climate sensitivity for NPP estimates from all but three TBMs. However, analyses of growth from tree-ring data and analyses of NPP from TBMs produced contrasting evidence concerning the key climate variables limiting growth. While analyses of NPP primarily indicated a positive relationship between growth and seasonal temperature, tree-ring analyses indicated negative growth relationships to temperature. Also, the positive effect of precipitation on NPP derived from most TBMs was weaker than the positive effect of precipitation on tree-ring based growth: temperature had a more important limiting effect on NPP than tree-ring data indicated. These mismatches regarding the key climate variables limiting growth suggested that characterization of tree growth in TBMs might need revision, particularly regarding the effects of stomatal conductance and carbohydrate reserve dynamics.

1. Introduction

Boreal forests store about 53.9 Pg of carbon, which is nearly 14 % of global terrestrial vegetation biomass (Pan et al., 2011). Forest productivity, a proxy for inputs associated with the forest capacity to store carbon, varies over the boreal/hemi-boreal zones due to regional variation in temperature and precipitation, as well as regional-to-local differences in vegetation, soils, surficial geology, and forest disturbance regimes (Brandt et al., 2013). In the context of climate change, the boreal/hemi-boreal zones, which are dominated by cold-tolerant tree species (Brandt et al., 2013; Girardin et al., 2021), are warming faster (0.5 °C per decade) than any other land area (Gauthier et al., 2014). As the climate continues to change, productivity of these forests is also expected to change due to increased drought severity and an increase in the frequency of major disturbance events such as fire, disease epidemics, and insect outbreaks (Serreze et al., 2000; Gauthier et al., 2014). Given regional variability of environments across the boreal forest, variable forest productivity responses to changes in climate are also expected. Increasing temperatures and changes in precipitation regimes are expected to impair forest growth in the western regions of the boreal forest, because of water stress deleterious for tree growth, but increase forest growth in the north-east (*i.e.* near the Great Lakes) where temperature is currently the main factor limiting growth (Price et al., 2013; Girardin et al., 2016a; Wulder et al., 2020). However, large uncertainties that plague our understanding of forest carbon dynamics reduce our capacity to predict forest growth responses to spatial and temporal variations in climate (Evans et al., 2022). Moreover, disentangling differential growth sensitivity to the same climate variations among regions of the boreal/hemi-boreal zones is challenging. Nevertheless, addressing these challenges will improve predictions about the impact of climate change on forest productivity. Such improvement would help design land management policies and strategies to mitigate the impacts of climate change on a range of ecosystem services, including carbon sequestration, the maintenance of biogeochemical cycles, and global climate regulation.

A significant portion of our knowledge about climate change impacts on forest productivity comes from terrestrial biosphere models (TBMs). TBMs simulate the physical, chemical and biological processes of terrestrial ecosystems across multiple spatial and temporal scales. They can represent biochemical pools and fluxes, and scale them at tree, stand and ecosystem level to predict vegetation dynamics influenced by temperature, precipitation, atmospheric moisture, and other climate features (Brandt et al., 2013; Bonan, 2019). TBMs are sophisticated tools that predict how forests could respond to changing climatic conditions and how these changes will, in turn, affect the Earth's system *via* gas, water and carbon fluxes (King et al., 2011; Huntzinger et al., 2013; Kolus et al., 2019). Specifically, forest growth-climate relationships in TBMs are based on the formulation of physiological processes and their responses to environmental factors. For instance, they simulate physiological processes such as tree growth responses to growing season length, photosynthetic changes during drought, or temperature-driven variations in carbon allocation among different plant parts. Among TBMs, predictions of forest productivity can be highly variable for some regions, or they may display systematic biases, which becomes evident when comparing model outcomes to observed growth. The formulation of physiological processes defining forests growth-climate relationships and their parameterization remains a major source of uncertainty in TBMs predictions of forest productivity (Babst et al., 2018; Zuidema et al., 2018; Friend et al., 2019). Additionally, these models might not capture some important ecological processes. For instance, growth predictions based on short-term responses to climate might not adequately represent the time lag between carbon assimilation and investment in tree growth, which has been observed for several species at various locations (Teets et al., 2018; Lagergren et al., 2019; Metsaranta et al., 2021; Cabon et al., 2022). TBMs also often differ in their mechanistic representation of stomatal conductance, rooting depth and spatial distribution, and the presence of carbohydrate reserve pools (Huntzinger et al., 2013). Therefore, evaluating TBMs by comparing their predictions and confronting them with observed tree growth data is relevant and timely, given the rapid developments underway to improve TBMs parameterization (Blyth et al., 2021; Wang et al., 2021; Fisher et al., 2022).

Field-based estimates of tree growth sensitivity to temperature and precipitation across regions are essential to refine the understanding of processes underlying forest responses to climate, to assess TBMs representativeness of climate responses and quantify predictions uncertainty, and to guide future model development (Medlyn et al., 2015; Klesse et al., 2018). Observational datasets from field studies should have high temporal resolution, occur over decades, and encompass large spatial extents to accurately estimate growth-climate relationships and capture their differences among regions, species and ecoclines over time (Klesse et al., 2018). In that respect, tree-ring data from large-scale sampling networks are ideal; they provide long-term *in situ* records of interannual radial tree growth variability, which is linked to both total stem and stand-level productivity in boreal Canada, including eddy covariance estimates of carbon fluxes and normalised difference vegetation indices (Girardin et al., 2014; Wettstein et al., 2011; Metsaranta et al., 2018, 2021). Such field observations from Canadian boreal forests have already showed variation in growth-climate relationships among regions (*e.g.*, maritime *vs.* continental), as well as among tree species (Breitenmoser et al., 2014; Marchand et al., 2021). Tree-rings strengthen the empirical foundation for improving forest productivity modelling and scaling of carbon dynamics from leaf to globe. They also form an obvious basis for benchmarking the capacity of models to anticipate climate effects on forests, in the sense of evaluating their performance compared to observed data (Girardin et al., 2016a; Klesse et al., 2018; Evans et al., 2022).

We compared the climate sensitivity of forest growth in the boreal/hemi-boreal zones of Canada, estimated from tree-ring network, to the climate sensitivity of net primary productivity (NPP), simulated by an ensemble of TBMs. This “benchmarking” of TBMs was achieved using a new Canada-wide network of tree-ring measurements from the nine most abundantly sampled (and dominant) species in the boreal/hemi-boreal zones of Canada (Girardin et al., 2021). We quantified annual growth changes in tree basal area increment as a function of seasonal temperature and precipitation fluctuations between 1950 and 2018 using multi-species linear mixed models. These estimated growth-climate relationships at the tree community level allowed us to map forests growth sensitivity to climate across Canada's boreal/hemi-boreal zones. These observed spatial patterns of growth sensitivity to climate variability were then compared to patterns of NPP sensitivity to climate variability predicted using an ensemble of simulations from 14 TBMs that are part of the Multi-scale Synthesis and Terrestrial Model Intercomparison Project (MsTMIP) (Huntzinger et al., 2013). These TBM simulations base on a common standardised climate forcing dataset with constant atmospheric carbon

dioxide concentration ([CO_2]), land use, and nitrogen deposition (Wei et al., 2014). Although a benchmark of TBMs representativeness of climate sensitivity has been realised using tree-ring data (*e.g.*, Tei and Sugimoto, 2020), our study is the first to undertake such an ensemble-model comparison over the entire Canadian boreal/hemi-boreal forests.

2. Methods

2.1. Study area

The study area encompasses the full extent of Canada's boreal forests, which we delineate as the boreal and hemi-boreal zones defined by Brandt et al. (2013). The climate in the boreal/hemi-boreal zones is predominantly high-latitude continental, with long cold winters, short cool summers, and relatively low annual precipitation, but with significant regional variation (Price et al., 2013). Eleven ecozones delineated across the boreal/hemi-boreal forests represent this regional variability (Ecological Stratification Working Group, 2016) (Fig. 1). These ecozones include the Montane Cordillera, Boreal Cordillera and Taïga Cordillera that contain the Canadian Rockies, the Boreal Plains and Taiga Plains located east of the Rockies, and Taiga Shield, Boreal Shield and Hudson Plains in the continental interior to the east. Bounded by three Great Lakes in the east is the Mixedwood Plains, and adjacent to the east coast is the Atlantic Maritime (Fig. 1). Average summer air temperature in boreal/hemi-boreal forests range from 10.0 °C in the Taiga Cordillera to 14.0 °C in the Atlantic Maritime ecozone and average winter air temperature range from −22.0 °C in the Taiga Cordillera to −1.5 °C in the Boreal Cordillera. Total annual precipitation (mm) average from 200 to 500 mm in the Taiga Plains to over 4000 mm in the Boreal Cordillera.

2.2. Tree-ring data

Annual tree-ring width data for the boreal/hemi-boreal forests were retrieved from the Canadian Forest Service Tree-Ring repository (CFS-TRenD 1.0; Girardin et al., 2021). CFS-TRenD contains width measurements from 40,206 tree samples from 4594 sites and 57 tree species collected across all Canadian provinces and territories. It was developed with the goal of combining data from different sources and making them available in a consistent format for large-scale analyses of tree growth. The primary national-scale tree-ring dataset in CFS-TRenD 1.0 comes from increment cores sampled since 2001, the establishment of Canada's National Forest Inventory (NFI). The NFI network, designed to represent species distributions and their range of growing conditions in Canada, comprises 6010 core samples from 870 sites (Gillis et al., 2005). Other tree-ring data come from more regional projects including data from permanent sample plots established by the Alberta Biodiversity Monitoring Institute (ABMI), temporary sample plots established by the ministère des Ressources naturelles et de la Faune du Québec (MFFPQ; Programme d'inventaire écoforestier nordique, Létourneau et al., 2008; Girardin et al., 2021), and the Climate Impacts on Productivity and Health of Aspen (CIPHA) network (Hogg et al., 2005). Several additional contributions to CFS-TRenD came from smaller-scale projects carried out by individual researchers, including datasets extracted from the International Tree-Ring Data Bank (ITRDB).

We limited our analyses to the dominant species in the dataset (Fig. 1) to maintain the accuracy and confidence of the statistical analyses *i.e.,* a sampling density for each species that balances local variations in growth across sampling sites within regions, and detects growth sensitivity to climate at regional scale. We analysed tree-ring data for nine species, seven genera and 32,189 trees, which represents 80 % of samples contained within the CFS-TRenD repository: *Picea mariana* (black spruce; 25 % of the dataset with 1.0 e^4 trees sampled), *Picea glauca* (white spruce; 12 %, 4.7 e^3 trees), *Pinus banksiana* (jack pine; 11 %, 4.4 e^3 trees), *Populus tremuloides* (trembling aspen; 10 %, 3.9 e^3 trees), *Pinus contorta* (lodgepole pine; 7 %, 2.9 e^3 trees), *Pseudotsuga menziesii* (Douglas fir; 7 %, 2.8 e^3 trees), *Picea engelmannii* (Engelmann spruce; 4 %, 1.7 e^3 trees), *Abies lasiocarpa* (subalpine fir; 2 %, 9.3 e^2 trees), and *Pinus resinosa* (red pine; 2 %, 8.7 e^2 trees). We excluded *Abies balsamea* (balsam fir, mostly dominant in the eastern ecozones) because its growth dynamics are strongly influenced by spruce budworm (*Choristoneura fumiferana*) defoliation (Lavoie et al., 2019; Sánchez-Pinillos et al., 2019). All of the nine species occur in Canadian boreal/hemi-boreal forests (Brandt et al., 2013). Forty two percent of the sites included two or three trees, and 83 % of the sites had data for a single species. Fifty percent of the trees displayed between 40 and 90 tree-rings. Both visual and statistical quality control procedures were applied to ensure that only true growth rings were measured and the correct calendar year was assigned to each tree-ring (Girardin et al., 2021). In an analysis of sample coherency, Girardin et al. (2021) found high spatial synchronicity in the interannual growth fluctuations among most samples. Only 12 % of samples had low coherence, and they were mainly non-boreal angiosperm species excluded from our analyses.

2.3. Model ensemble simulations

NPP simulations were retrieved from the MsTMIP v1 ensemble of terrestrial biosphere model simulations generated by the North American Carbon Program (*NACP*, https://daac.ornl.gov/cgi-bin/dsviewer.pl?ds_id=1225; Huntzinger et al., 2013; Wei et al., 2014). MsTMIP defines a set of sensitivity simulations designed to isolate the impact of different drivers (climate, atmospheric carbon dioxide concentration, land cover change history, and nitrogen deposition) on simulated variables (*e.g.*, carbon and energy fluxes, carbon pools) (Kolus et al., 2019). The MsTMIP system ensures that protocols are run consistently across models, user decisions on forcing data are systematic, there is no tuning, and that output is saved, transferred, and analysed uniformly. We used 14 models: BIOME-BGC, CLASS-CTEM-N+, CLM4, CLM4-VIC, DLEM, GTEC, ISAM, LPJ-wsl, ORCHIDEE-LSCE, SiB3, SiBCASA, TEM6, VEGAS2.1, and VISIT (see Table S1 for model attributes related to energy flux formulation and parameterization). These models were recently run with a suite of climate and RCP projections (Fisher et al., 2022). Our objective was to evaluate the sensitivity of models predictions to climate fluctuations. Accordingly, we used the model outputs corresponding to the climate-varying sensitivity simulations (SG1), where atmospheric carbon dioxide concentration, land use, and nitrogen deposition are all held constant within this SG1 ensemble. We retrieved simulated outputs providing global gridded estimates of NPP at monthly and yearly time steps for the period 1900 to 2010, with a spatial resolution of 0.5 × 0.5°. For the purpose of our analyses, we associated NPP values of grid cells with growth values from tree-ring sampling sites located within 60 km of the cell. In addition to NPP outputs, we also retrieved annual above ground biomass outputs for the five TBMs for which these data were available: BIOME-BGC, CLM4, CLM4-VIC, GTEC, and SIBCASA. These outputs were converted into annual aboveground wood biomass increments (AGW).

2.4. Climate dataset

Temperature and precipitation are key climatic drivers of vegetation productivity (Zscheischler et al., 2014). We obtained daily maximum and minimum temperature (°C), precipitation (mm) and relative humidity (%) for the period from 1950 to 2018 using the BioSIM v11 software, which interpolates site-specific estimates from Environment Canada historical weather observations (Régnière and Bolstad, 1994; Régnière et al., 2014). The daily data were interpolated to a 1° x 1° grid (n = 604 grid cells). From the daily weather estimates, BioSIM calculates vapour pressure deficit (VPD, in KPa), the difference between the actual atmospheric water vapour amount and the maximum water vapour amount at saturation for a given temperature. BioSIM also calculates a soil moisture index (SMI, in mm), using a quadratic-plus-linear formulation procedure (Hogg et al., 2013) based on water lost by evapotranspiration and gained from precipitation. Also, for each grid cell, seasonal means of daily mean temperature and sum of precipitation were computed from winter season (December to February), spring (March to May), summer (June to August), and autumn

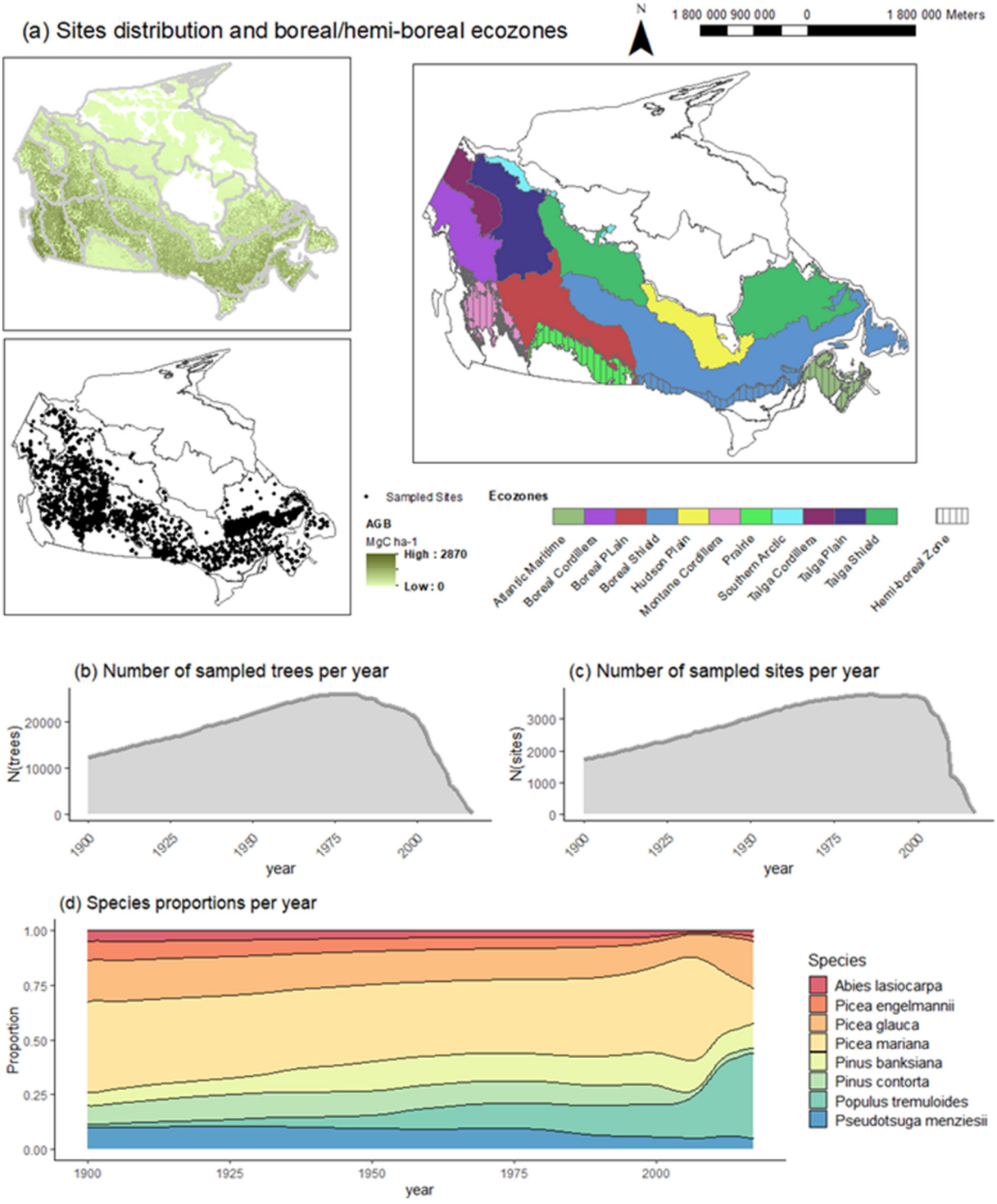

Fig. 1. Description of tree-ring dataset. (a) Distribution of sample sites. The background colour on the map at left illustrates the distribution of the aboveground biomass (AGB) across Canada's forests (Spawn and Gibbs, 2020): the distribution of sample sites for the tree-ring dataset encompassing the nine sampled species is represented by black points. Canadian Ecozones are illustrated on the map at right, within the boreal/hemi-boreal (hatched) zones. Yearly temporal distributions of sampled (b) trees, (c) sites, and (d) species proportions.

(September to November) (Trenberth, 1983). We calculated these variables up to autumn of the current year which marks the end of cell-wall lignification, as shown for black spruce (Rossi et al., 2012). The climate variables of the closest grid's centroid were assigned to each tree-ring sampling site. Cross-correlation between BioSIM interpolated observations and CRUNCEP climatology used in the MsTMIP ensemble indicated high consistency between both datasets (Table S2). Therefore, we conducted our analyses using BioSIM output, which offers more flexibility for interpolation and in the types of climate variables that can be extracted. Sensitivity analyses using CRUNCEP data are provided in Supplementary Materials.

2.5. Detrending of tree-ring data

Time series of annual ring-width were converted into time series of yearly basal area increments (BAI; $cm^2\ yr^{-1}$), because basal area increment

is more closely related to tree productivity than ring width (Babst et al., 2014b). When multiple radii of ring-width measurements were available for a particular tree, they were first averaged at the tree level. BAI was estimated from:

$$BAI_t = \pi R_t^2 - \pi R_{t-1}^2 \quad (1)$$

where R_t and R_{t-1} are the stem radii (cm) at the end and beginning of an annual ring increment. Minimum tree age was determined from ring counts, starting from the outermost ring. Because very early tree growth is much different from growth in later development stages, we excluded tree-rings formed during the first ten years for each time series in the following analysis of tree growth-climate relationships (Loader et al., 2007).

Time series of annual basal area increment were detrended to remove growth trends due to tree development stage (Zhang et al., 2018). Detrending was implemented using generalised additive mixed models (GAMM) fitted to the log-transformed BAI series at each site (4006 models), with tree considered as a random effect:

$$log\left(BAI_{ijkt}\right) = \beta_{kj}.\ log\left(BA_{ijk(t-1)}\right) + s\left(age_{ijkt}\right) + TreeID_{ijk} + corAR1_{ijk} + \epsilon_{ijkt} \quad (2)$$

where *i* stood for tree identity, *j* for the species, *k* for the site, and *t* for the year. *BAI* was the basal area increment of tree *i* at year *t* and *age* was its age in year at time *t*, *BA* was the basal area, and *TreeID* was a unique identifier. Temporal autocorrelation was considered with *AR1*, an autoregressive term of order 1, and the smoothing parameter *s* was a cubic regression spline. The growth model was fitted using the mgcv R package (Wood, 2006). The residuals $BAI\{Resid.\}_i$ from these GAMM models, which represented the growth variations unrelated to tree development stage, were the detrended series (Girardin et al., 2016b) used in the following analyses.

2.6. Sensitivity of tree growth and NPP/AGW to climate variability

Both tree growth-climate relationships and NPP-climate relationships were determined by linear mixed models. For BAI, multi-species (community-level) models were employed and took on the form:

$$BAI\{Resid.\}_i = \sum_k \beta_k Clim_k^t + species_j + corAR1_{ijk}^t + \epsilon_{ik}^t \quad (3)$$

where $BAI\{Resid.\}_i$ were detrended BAI series averaged by species *j* at site level *i*, *k* was the climatic variable, *t* was the year, and *AR1* was an autoregressive term of order 1. Hence, one model was conducted for each site, with each species present at that site being represented by the random effect *species*. The complete model considered 12 climate variables including precipitation and average air temperature for the four seasons of the year of growth, plus the previous-year summer and autumn precipitation and temperature (Babst et al., 2014a; Girardin et al., 2016b). From this complete model, a set of best fitting models, only including the most significant variables, was selected through multi-model selection based on the Akaike Information Criterion (AIC) using the MuMIn R package (Barton and Barton, 2015). All models for which cumulative Akaike weight remained below 0.95 were retained to constitute a 95 % confidence interval set of models (Burnham and Anderson, 2002). Climate variables estimates were averaged among selected models and weighted by models AIC. The statistical significance of these estimates was computed *via* Student *t*-statistic using a ratio of the estimate to its standard deviation. Climate variable importance value was computed as sum of AICs for all models in which a climate variable had a significant effect on BAI, and then multiplied by the sign of the estimate to maintain the sign of the relationship between BAI and the climate variable. We repeated this linear mixed model procedure on the output of 14 TBMs, using annual NPP summed over a window from January to December as the dependent variable. Here, a linear mixed model relating NPP to the seasonal climate variables (as in Eq. (3), but removing the *species* term) was conducted for each of the grid cells assigned to the tree-ring sampling sites (Section 2.4), with the procedure repeated for each of the 14 TBMs. We also conducted sensitivity analyses on NPP summed over a window stretching from previous July to June, and on annual (January to December) AGW. It should be noted that in TBMs, plant functional types (PFTs) are used to represent the response of vegetation dynamics. In this case, the effects of climate variability are typically simulated as an increase or decrease in the share of NPP/AGW in a given PFT. The sum of the NPP/AGW values on a grid cell should therefore be considered as a community-level quantity. Since we used the multi-species (community-level) GAMM to derive climate sensitivity, we assumed that the community-level NPP/AGW was comparable to the information derived from the multi-species tree-ring models.

We compared the climate sensitivity of forest growth in the boreal/hemiboreal zones, estimated from BAI, to the climate sensitivity of NPP simulated by each of the TBMs. To make this comparison, we needed to address the paucity of climate stations and tree-ring data in northern forests, which could cause data interpolation processes to excessively smooth climate and growth data (*i.e.*, with low variability across space). This may dampen the importance of climate variable estimates in models of basal area increment (Ols et al., 2018). Conversely, higher importance of seasonal climate in models using NPP/AGW can logically emerge from the calculation alone, since NPP/AGW are themselves calculated from climate data. To correct for these effects, an importance weighted mean (IWM) was calculated for each seasonal climatic variable of NPP or BAI. The unitless IWM metric is defined by the sum across sites of climatic variable importance values, weighted by the frequency of time the variable is significant at the 5 % level, and normalised by the maximum IWM for each association:

$$IWM^{pm} = \sum_{Sites} Imp_i^{pm} * \left(N_{Significant\ Sites} / N_{Sites}\right) \quad (4a)$$

$$IWM_{Norm}^{pm} = {}^{IWM^{pm}} \Big/ {}_{max\left(\{IWM^{pm}\}_{Variables}\right)} \quad (4b)$$

where IWM^{pm} is the relative importance of climate variable *p* from the output of model *m*, *i.e.* either BAI-climate or NPP-climate, Imp_i^{pm} is the importance of climate variable *p* from the output model *m* at site *I*, $N_{Significant\ Sites}$ is the number of sites where climate variable *p* from the output of model *m* is significant, and max is maximum importance values obtained for climate variable *p* from the output model *m*.

For the BAI and NPP models, we assessed the strength and direction of the sensitivity to climate with the sum of temperature-related ($Temperature_{Index}$) and precipitation-related ($Precipitation_{Index}$) importance at the site level, *i.e.,* the sum of selected model AICs where any temperature/precipitation variable was significant:

$$Temperature_{Index} = \Sigma_{i=1}^{n} imp_i * sign(est_i) \quad (5a)$$

$$Precipitation_{Index} = \Sigma_{i=1}^{n} imp_i * \ sign(est_i) \quad (5b)$$

$Temperature/Precipitation_{Index}$ measures site growth/NPP dependency on energy conferred by temperature, and dependency on water conferred by precipitation, and *n* is the number of significant seasonal temperature or precipitation climate variables. Site-level climatic sensitivity indices ($Climate_{Index}$) were computed as the difference between $Temperature_{Index}$ and $Precipitation_{Index}$.

$$Climate_{Index} = Temperature_{Index} - Precipitation_{Index} \quad (6)$$

A negative $Climate_{Index}$ indicated higher sensitivity to precipitation than to temperature, so high water limitation and low thermal limitation on growth, *i.e., related to the effect of heat increase.* A positive $Climate_{Index}$ indicated higher temperature than precipitation sensitivity, so high thermal and low water growth limitation (Babst et al., 2019). To determine if there were any specificities in the results induced by the presence of particular species, we closely examined the $Climate_{Index}$ of the five most abundant species in the tree-ring dataset and mapped the corresponding species-specific sensitivity for four coniferous species, *Picea glauca, Picea mariana,*

Pinus banksiana, *Pinus contorta*, and one deciduous species, *Populus tremuloides*. These five species represent 2.6 e^4 trees, and 64 % of the total sampled trees in the tree-ring database.

2.7. Mapping growth sensitivity to climate

$Temperature_{Index}$, $Precipitation_{Index}$, and $Climate_{Index}$ were locally interpolated using bilinear inverse distance weighting (*IDW*) interpolation with a 0.1° resolution and a 12-points search radius. Interpolation was performed using ArcGIS, version 10.6 (ESRI, ArcGIS Desktop, 2011). Results for the boreal/hemi-boreal zones (Fig. 1, Brandt et al., 2013) were extracted from the output raster layers.

We assessed the capacity of TBMs to reproduce spatial patterns in sensitivity to climate variations by correlating the spatial vector (*i.e.*, map) of $Climate_{Index}$ produced from NPP simulated by each TBM to the maps produced from analysis of BAI data. We performed the correlation test on interpolated $Climate_{Index}$ values across interpolation grid cells, to balance the differences in sampling sites density among regions. The degrees of freedom (df) for the *t*-test were corrected for the presence of spatial correlation using the methodology described by (Dutilleul et al., 1993). The analysis was performed using the R package 'SpatialPack' (Vallejos et al., 2020). The null hypothesis, that 'TBM does not reproduce the observed pattern', was rejected when $p > 0.05$.

2.8. Correlation with terrestrial biosphere models

The relationship between NPP simulated by TBMs and BAI obtained from tree-ring data collected at the closest sampling site, was estimated using GAMMs fitted for each site and each terrestrial biosphere model (1388 models):

$$BAI\{Resid.\}_i = \beta_m NPP^t_{mi} + s\left(age^t_{ij}\right) + corAR1^t_{jk} + Species_j + \epsilon^t_{ij} \quad (7)$$

where $BAI\{Resid.\}_I$ is the observed growth residuals for site *i*, *m* is the vegetation model, *t* is the year, *j* is the species, and *AR1* is an autoregressive term of order 1. To measure vegetation model performance, we computed the Pearson square-correlation between observed and predicted growth at each site.

2.9. Separating temperature effects on growth from effects of vapour pressure deficit and soil moisture

The effects of temperature on growth originate from multiple mechanisms affecting photosynthesis and reflect the effects of the lengthening of the growing season, frost, soil water availability, and atmospheric water demand. Separating the contribution of some of these covariates could provide a better understanding of the factors driving the temperature limitation observed in the BAI data. Accordingly, we re-examined the seasonal temperature and growth relationship whilst taking away the effects of covariates, *e.g.*, soil water availability (SMI) and atmospheric moisture content (VPD), on this relationship. For the sites displaying significant growth-climate relationship (3978 sites), we fit a generalised least squares model describing site-level detrended growth in relation to local SMI and VPD of the current and previous years. For the sites with more

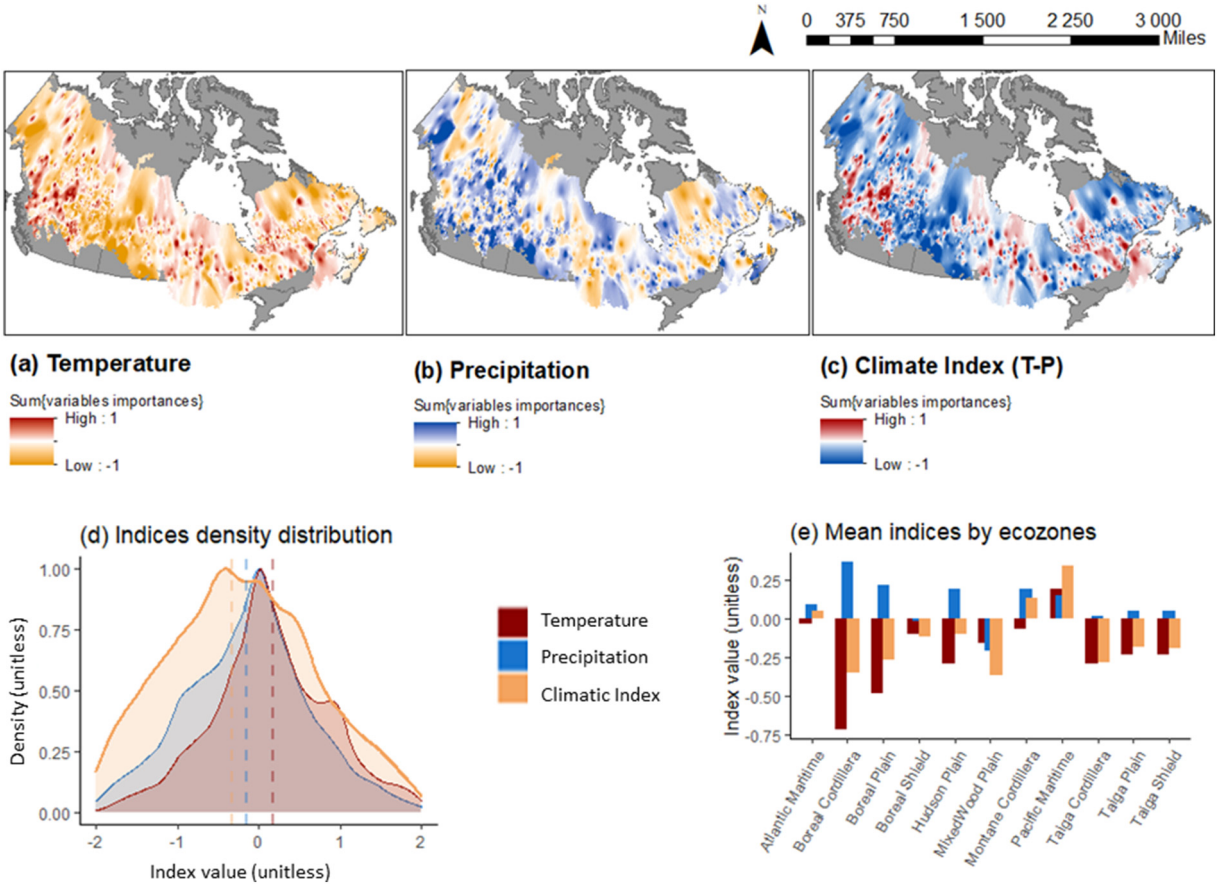

Fig. 2. Temperature, precipitation and climate sensitivity indices in the boreal/hemi-boreal zones estimated for twelve climatic variables from basal area increments. (a) Temperature related importance (T), with energy-limited sites responding positively to temperature. (b) Precipitation related importance (P), with water-limited sites responding positively to precipitation. (c) $Climate_{index}$, the difference between T and P. Positive $Climate_{index}$ indicates temperature effects (energy limitations) are greater than precipitation effects (water limitations), while negative values indicate the opposite. (d) The density distribution of T, P, and $Climate_{index}$, dashed lines representing the means. Bidimensional interpolation was performed on a spatial resolution of 0.1 × 0.1°, using the inverse distance weighting method based on the 12 closest neighbours. The density distributions of climate sensitivity indices (unitless) are displayed at bottom. (e) Mean values of T, P, and $Climate_{index}$ by ecozone.

than one tree species, we fit a linear mixed model with a random effect for each species, with a first-order autocorrelation parameter (AR1):

$$BAI\{Resid.\}_i = \alpha_i^1 SMI_i^t + \alpha_i^2 SMI_i^{t-1} + \beta_i^1 VPD_i^t + \beta_i^2 VPD_i^{t-1} + corAR1_i^t + \epsilon_k^t \quad (8)$$

where $BAI\{Resid.\}_i$ is the growth residuals for site i (see Eq. (3)), and t stands for the year of growth. The residuals of this model ($BAI_{/SMI+VPD}\{Resid.\}_i$) were related to summer temperature and previous summer temperature using a generalised least square model, with a first-order autocorrelation parameter:

$$BAI_{/SMI+VPD}\{Resid.\}_i = \alpha_i^1\ SummerTemp._i^t + \alpha_i^2\ SummerTemp._i^{t-1} + corAR1_i^t + \epsilon_k^t \quad (9)$$

The null hypothesis of no relationship between temperature and growth, independently of VPD and SMI, was rejected at the 5 % level (one-sided test) when $p < 0.05$. Results were reported as the percentage of sites for which temperature remained significant. To ensure no species effect persisted on the relationship between residuals and temperature variables, we ran this model on sites with single species only, and obtained similar results.

3. Results

3.1. Differential growth sensitivity to temperature and precipitation variability is related to region and species

We assessed the sensitivity of tree growth to climate variations from the Canada-wide annual tree-ring network retrieved from the Canadian Forest Service Tree-Ring repository (CFS-TRenD 1.0; Girardin et al., 2021). Across the nine most sampled tree species in the repository, *Picea mariana*, *Picea glauca*, *Pinus banksiana*, *Populus tremuloides*, *Pinus contorta*, *Pseudotsuga menziesii*, *Picea engelmannii*, *Abies lasiocarpa*, and *Pinus resinosa*, the average goodness-of-fit between year-to-year observed annual basal area increment (BAI) fluctuations and growth predicted from site-specific growth-climate models was $\overline{r2} = 0.22$ ($\sigma \pm 0.14$, $n = 4006$ linear mixed models; Fig. 2). Average goodness-of-fit was highest for sites populated by the genus *Pinus* ($\overline{r2} = 0.24$ with $\sigma \pm 0.19$, $n = 964$ linear mixed models; Fig. S1). Seasonal climate variables with the most significant impact on BAI were summer precipitation in the year prior to ring formation and mean summer temperature in the year prior to ring formation (Table 1). Previous summer precipitation was significantly positively related to BAI in 29 % of all models (for 1174 of the 4006 sites), indicating that above average summer precipitation enhanced annual tree growth the following year. Previous summer temperature was also significantly related to BAI, with a negative correlation for 34 % of all models (1373 sites), and a positive correlation in only 7 % of all models (279 sites), implying that warm summer temperatures impaired annual tree growth the following year. High precipitation and high temperature in the current summer had positive and negative impacts, respectively, on BAI but much less consistently than the effect of prior summer conditions.

Analyses of growth sensitivity to seasonal climate indicated strong, positive growth responses to increasing precipitation in the Boreal Cordillera, Taiga Plains and Boreal Plains, suggesting that growth at each site was constrained by the availability of water from precipitation (Fig. 2). Strong, positive growth responses to temperature occurred in southwestern Canada (the Montane Cordillera ecozone) and in eastern Canada (the Boreal Shield, Taiga Shield, Hudson Plains, and Atlantic Maritime ecozones), whereas a strong negative growth response to temperature was observed in the central-south portion of the country (the Boreal Plains ecozone), suggesting that growth at each site was constrained by the effect of temperature (Fig. 2). Differential growth sensitivities to climatic variations across forests of the boreal/hemi-boreal zones were particularly noticeable when aggregating these results into the climate index metric ($Climate_{Index}$), that is, the difference between the sums of temperature-related and precipitation-related importance values (see Section 2.6). A positive $Climate_{Index}$ meant

Table 1
Summary of predictors for (a) site-specific growth variability. Each value represents the number of times (with proportion indicated in parenthesis) a given variable was selected among the 4006 linear mixed models relating annual tree growth with seasonal climate variables, and for (b) simulated net primary productivity (NPP) variability from a suite of 14 terrestrial biosphere models (TBMs).

		Previous Summer Precipitation	Previous Summer Temperature	Previous Autumn Precipitation	Previous Autumn Temperature	Winter Precipitation	Winter Temperature	Spring Precipitation	Spring Temperature	Summer Precipitation	Summer Temperature	Autumn Precipitation	Autumn Temperature
(a) Growth - climate	Positive	1174 (29 %)	279 (7 %)	576 (14 %)	527 (13 %)	537 (13 %)	719 (18 %)	643 (16 %)	740 (18 %)	709 (18 %)	534 (13 %)	556 (14 %)	585 (15 %)
	Negative	326 (8 %)	1373 (34 %)	586 (15 %)	725 (18 %)	588 (15 %)	450 (11 %)	552 (14 %)	529 (13 %)	488 (12 %)	685 (17 %)	572 (14 %)	502 (13 %)
(b) NPP - climate	Positive	876 (17 %)	656 (13 %)	627 (12 %)	739 (14 %)	502 (10 %)	1031 (20 %)	892 (17 %)	3382 (65 %)	2122 (41 %)	2910 (55 %)	617 (12 %)	2451 (47 %)
	Negative	535 (10 %)	762 (15 %)	577 (11 %)	593 (11 %)	780 (15 %)	430 (8 %)	493 (9 %)	151 (3 %)	240 (5 %)	907 (18 %)	499 (10 %)	179 (3 %)

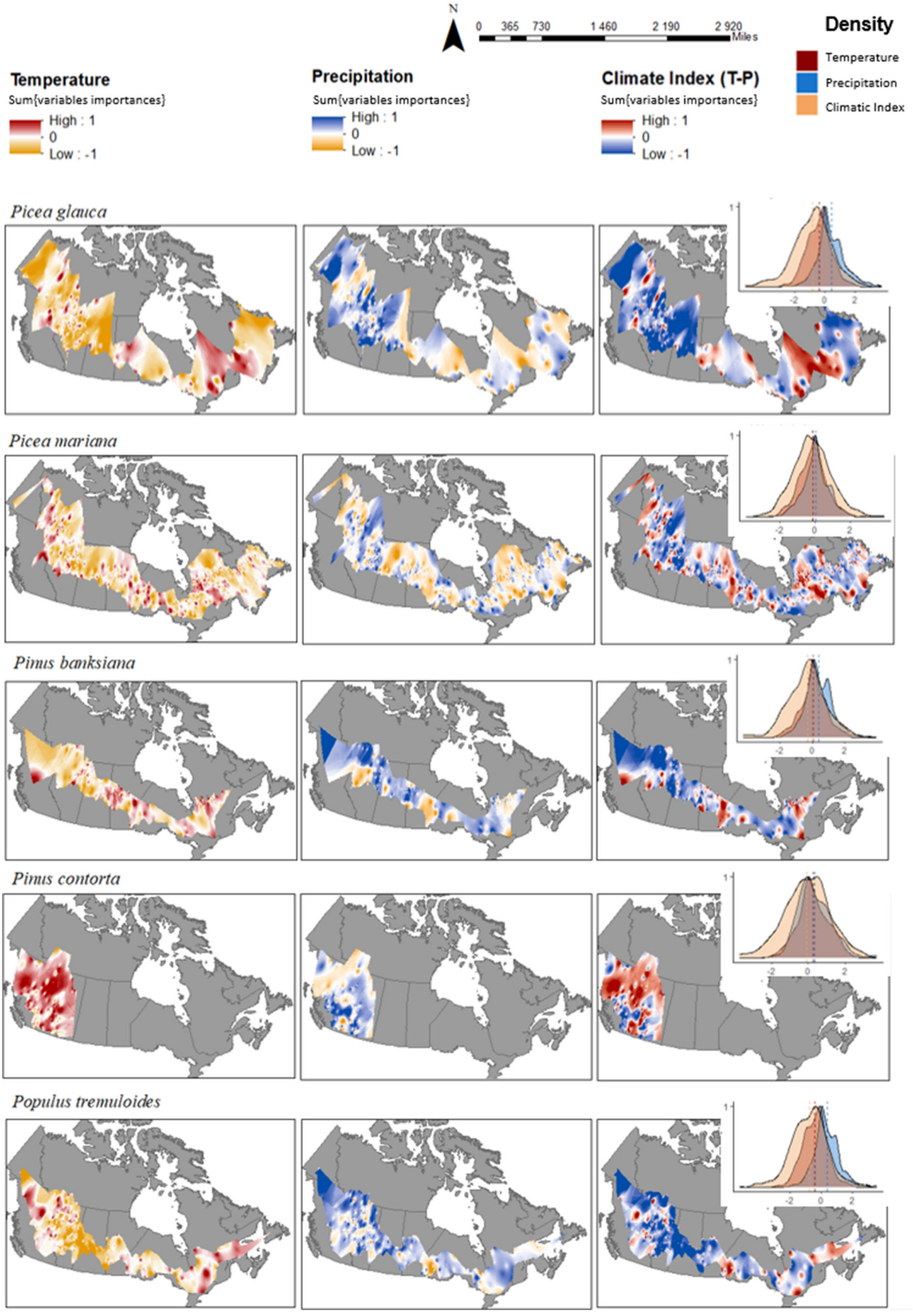
N
0 365 730 1 460 2 190 2 920
Miles
Density
Temperature
Precipitation
Climatic Index
Temperature
Sum{variables importances}
High : 1
0
Low : -1
Precipitation
Sum{variables importances}
High : 1
0
Low : -1
Climate Index (T-P)
Sum{variables importances}
High : 1
0
Low : -1
Picea glauca
Picea mariana
Pinus banksiana
Pinus contorta
Populus tremuloides

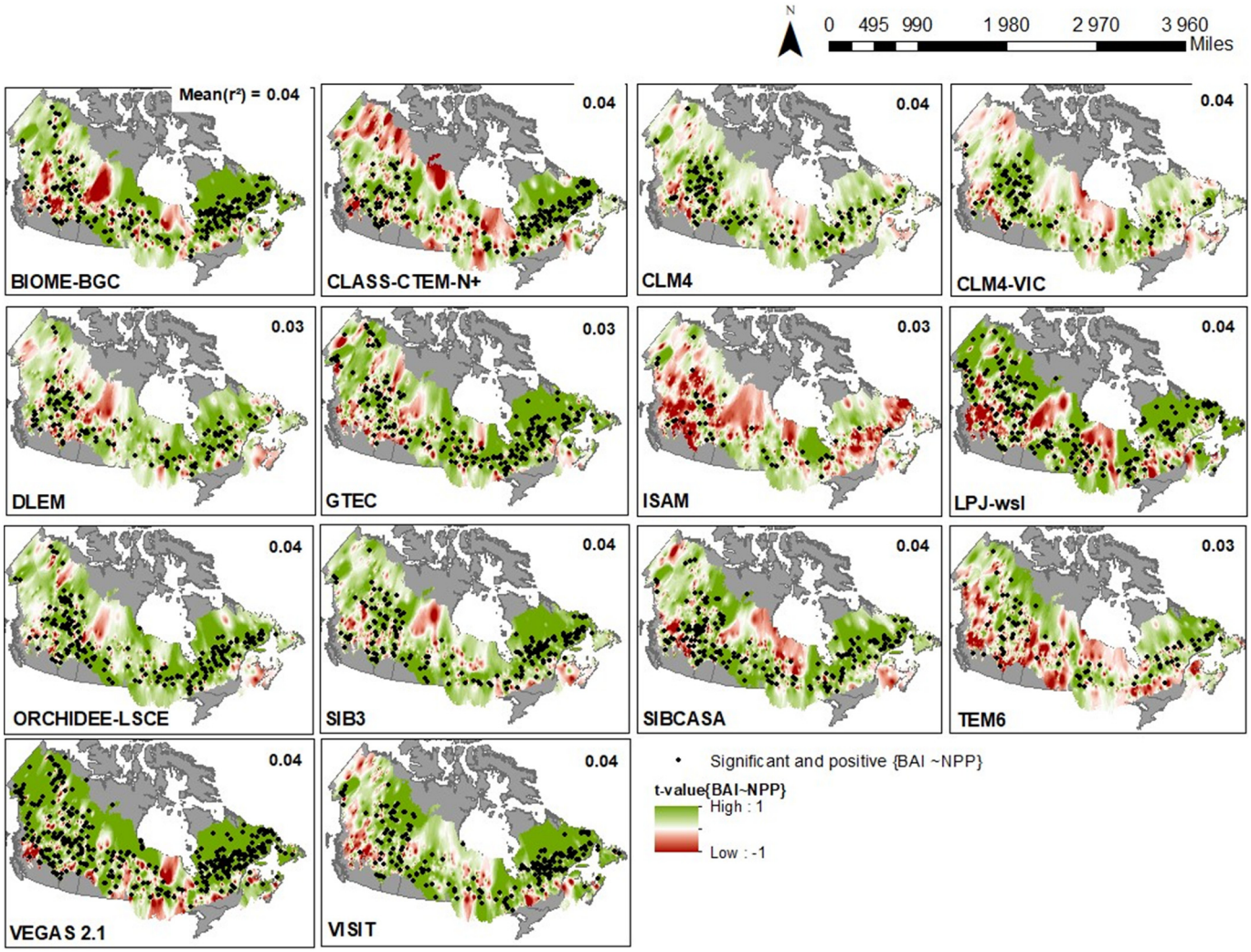

Fig. 4. Pointwise t-value of the regression between annual growth fluctuations estimated from tree-rings (BAI) and net primary productivity (NPP) fluctuations simulated by fourteen terrestrial biosphere models. Bidimensional interpolation, using all sampled sites, was performed on a spatial resolution of 0.1 × 0.1°, using the inverse distance weighting method based on the 12 closest neighbours. Black dots represent sites displaying positive and significant BAI-NPP correlation, at the one-sided 0.05 threshold. The average goodness-of-fit (r^2) across Canada of the BAI-NPP regression models are indicated for each terrestrial biosphere model.

a greater importance of the correlation between growth and temperature than between growth and moisture fluctuations. Overall, $Climate_{Index}$ was positive in parts of the Boreal Shield and Taiga Shield ecozones. This indicates that above average temperature, or below average precipitation, was beneficial to tree growth in these forests. $Climate_{Index}$ was negative in the Boreal Plains, Taiga Plains, and west of the Boreal Shield, signifying that high temperature, or low precipitation, was detrimental to growth in these ecozones.

Species-specific patterns of growth sensitivity to climate variables produced similar southwest-northeast patterns observed in the analyses of all species together (Fig. 3). However, *Picea glauca*, *Pinus banksiana*, and *Populus tremuloides* were more sensitive to moisture fluctuations than *Picea mariana* and *Pinus contorta* in the Boreal Cordillera, Taiga Plains and Boreal Plains.

3.2. Tree-rings and TBMs generate similar patterns of sensitivity to climate variability

The correlation between site-by-site time series of BAI and annual simulations of NPP showed, across the 14 TBMs evaluated, an overall goodness-of-fit averaging $\overline{r2} = 0.03$ ($\sigma \pm 0.03$, $n = 24{,}430$ models; Fig. 4). Across all TBMs, 16.1 % of the correlations between BAI and simulated NPP were significant (11.5 % positive, 4.4 % negative). The highest fits were in the Montane Cordillera, Taiga Plains, Boreal Plains and eastern Boreal Shield ecozones. The five TBMs with the highest percentage of positive correlations with BAI were VEGAS2.1 (21 % of tests), LPJ-wsl (17 %), SiBCASA (14 %), Biome-BGC (13 %), and ORCHIDEE-LSCE (13 %). Summing NPP over different time windows (*e.g.,* from summer prior to ring formation to the spring of ring formation) generated no

Fig. 3. Species-specific temperature, precipitation and climate sensitivity indices estimated from basal area increments. (a) Temperature related importance (T). (b) Precipitation related importance (P). (c) $Climate_{index}$, the difference between T and P. See Fig. 2 for definitions. Bidimensional interpolation was performed on a spatial resolution of 0.1 × 0.1°, using the inverse distance weighting method based on the 12 closest neighbours. The density distributions of climate sensitivity indices (unitless) are displayed on the corresponding inset.

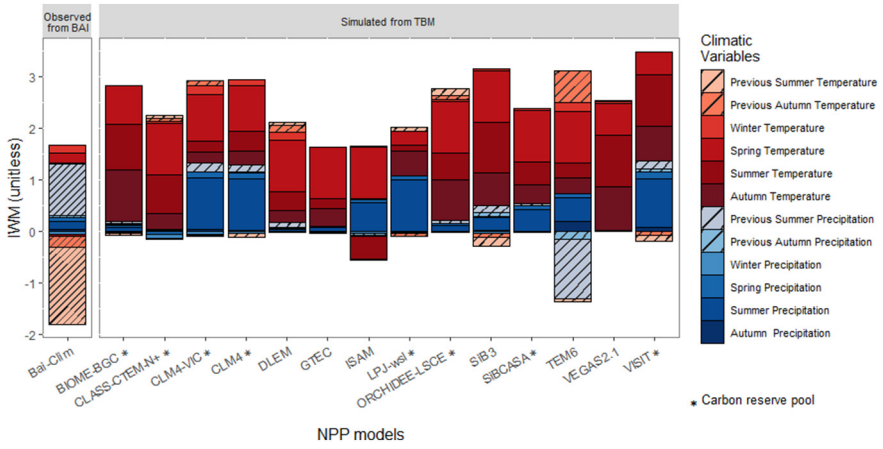

Fig. 5. Tree-ring and model comparison of seasonal temperature and precipitation sensitivities. Importance weighted means (IWM) of seasonal climate variables estimated from analyses of basal area increments (BAI-Clim) compared with the climate sensitivity of net primary productivity (NPP) simulations by an ensemble of fourteen terrestrial biosphere models (TBMs; at right). A positive IWM score indicates that the climate variable is beneficial to growth (or NPP); a negative IWM score denotes that the climate variable is detrimental. The seasons analysed range from the summer of the pre-growth year to the fall of the contemporary growth year. TBMs integrating a carbohydrate reserve pool are indicated.

difference in goodness-of-fit ($\overline{r2} = 0.04$, $\sigma \pm 0.05$, $n = 24{,}127$ models; Table S3).

We assessed the sensitivity to climate variability of NPP simulated by TBMs using linear mixed models relating NPP with the set of climatic variables. Across TBMs and sites, the average goodness-of-fit of the models was $\overline{r2} = 0.47$ ($\sigma \pm 0.17$, $n = 73{,}074$ models). Variables significantly influencing NPP were winter, spring, and summer temperatures, and spring and summer precipitation, all of which were positively correlated with NPP (Table 1 and Fig. 5; also see Fig. S2). Precipitation variables significantly influencing NPP were current summer precipitation for CLM4, CLM4-VIC, LPJ-wsl, and VISIT, and previous summer precipitation for TEM6 (Fig. 5). Average goodness-of-fit for the same analysis on AGW increment for the five TBMs where this variable was available was $\overline{r2} = 0.34$ ($\sigma \pm 0.16$, $n = 22{,}370$ models). Previous summer, summer and spring temperatures, and previous summer precipitation were significantly influencing AGW increment (Fig. 6). Comparing the importance values of climate variables between the TBM and BAI datasets, we found that neither TBM replicated the observed sensitivities of tree growth to climate variability exactly (Figs. 5 and S3). NPP and AGW from TBMs mainly displayed a positive relationship to seasonal temperatures, while BAI-climate models output showed mainly negative temperature relationships (Fig. 5). Such differentiation was accentuated when comparing the density distribution of $Climate_{Index}$ from NPP simulated by TBMs to that produced from BAI data (Fig. 7): there was an overestimation of the positive relationship with temperature, and hence of the importance of thermal limitation compared to moisture. The lagged sensitivity to climate noted in BAI was not observed in analyses of NPP, but was detected in analyses of AGW. Some of the TBMs incorporate, to some degree, a time lag in growth sensitivity to climate variations by integrating a carbohydrate reserve pool (Biome-BGC, CLM4, CLM4-VIC and SIBCASA). The TBM that did not consider a carbohydrate

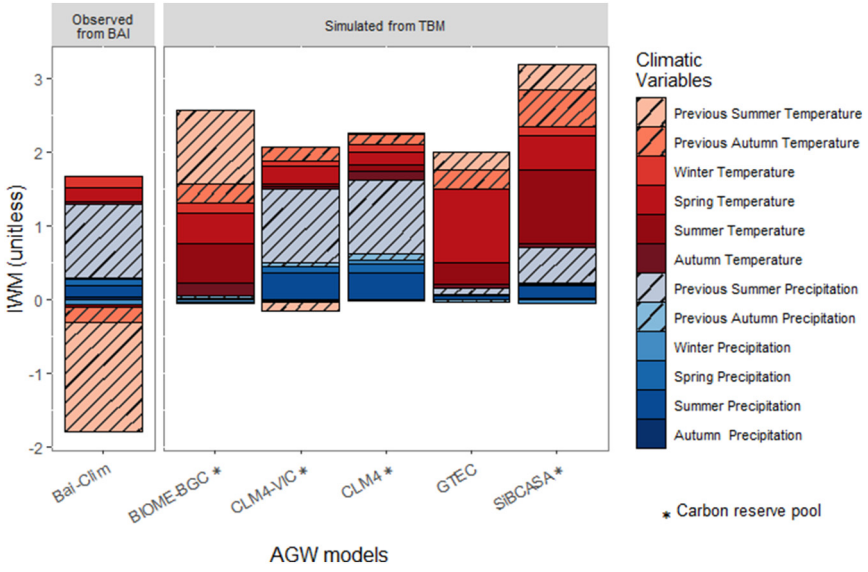

Fig. 6. Model comparison of seasonal temperature and precipitation sensitivities of aboveground wood biomass increments (AGW, sums of January to December) from an ensemble of five terrestrial biosphere models. Models displaying a carbon reserve pool are indicated with an asterisk. A positive IWM score indicates that the climate variable is beneficial to AGW; a negative IWM score denotes that the climate variable is detrimental. The seasons analysed range from the summer of the pre-growth year to the autumn of the contemporary growth year.

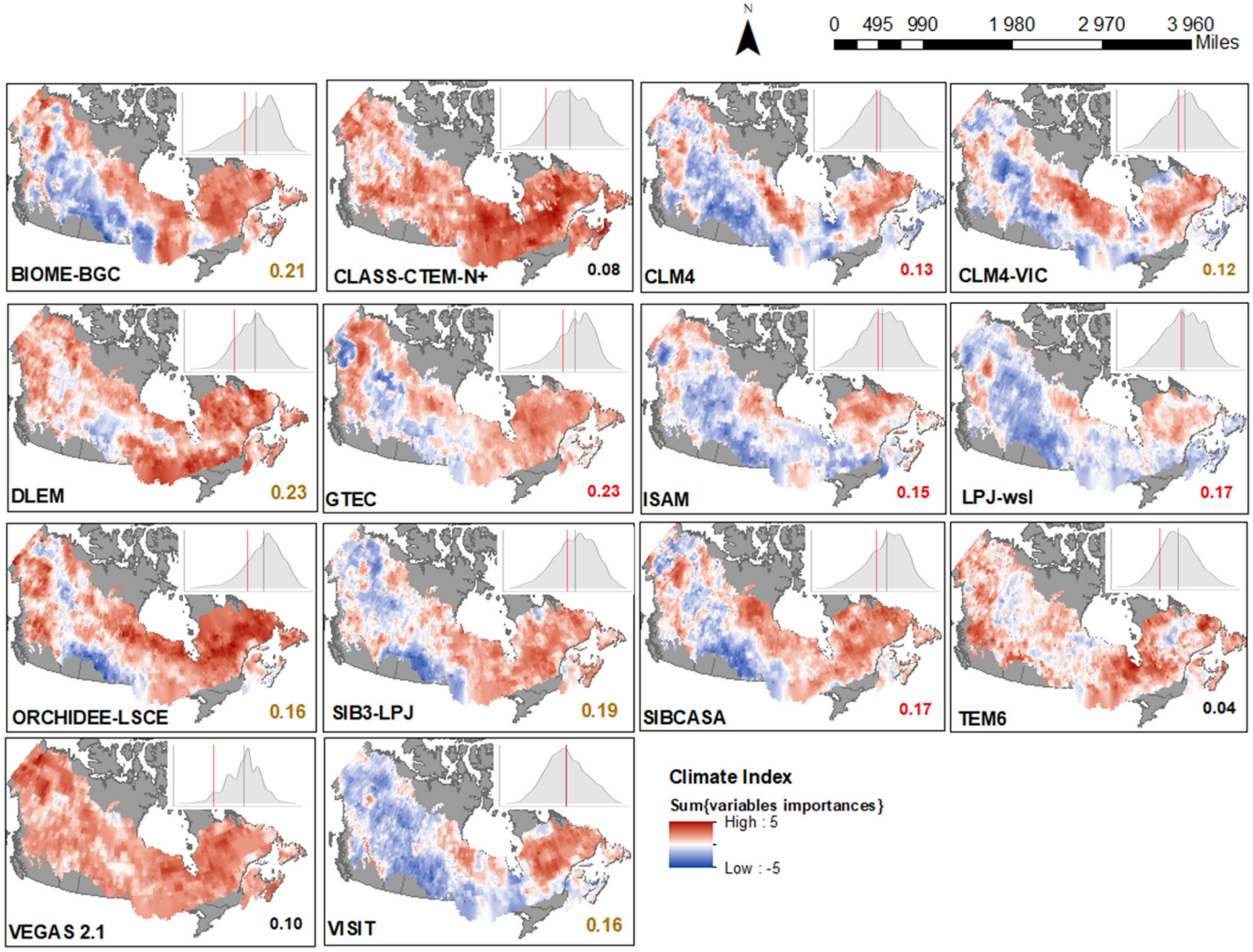

Fig. 7. Climate sensitivity indices in the boreal/hemi-boreal zones estimated from net primary productivity (NPP) fluctuations simulated by fourteen terrestrial biosphere models. Bidimensional interpolation was conducted on the climate sensitivity indices ($Climate_{Index}$) at a spatial resolution of 0.1 × 0.1°, using the inverse distance weighting method based on the 12 closest neighbours. The distributions of climate sensitivity indices probability density measured are displayed on the corresponding inset. On each map is also indicated the spatial correlation between the interpolated $Climate_{Index}$ estimated from the specified TBM with that from analyses of BAI (Fig. 2c). Correlations significant at a one-sided 0.05 threshold are indicated in red, and correlations significant at a one-sided 0.1 threshold are indicated in orange (the corresponding *p*-value and degree of freedom are displayed in Table S4).

reserve pool (GTEC) by default missed the lagged sensitivity to fluctuating climate (see Fig. S2).

Overall, correlations computed among the $Climate_{Index}$ maps indicated a significant capacity of simulations to reproduce spatial-temporal climate effects on growth in five TBMs ($p < 0.001$: CLM4, GTEC, ISAM, LPJ-wsl, and SiBCASA) and marginally significant in six TBMs ($p < 0.050$: Biome-BGC, CLM4-VIC, DLEM, ORCHIDEE-LSCE, SiB3-JPL, VISIT) (Fig. 7 and Table S4). The magnitudes of the *r* tests were small, however, with no >9 % of variance (r^2) in the climate sensitivity pattern being captured by the simulations. Three TBMs did not reproduce the observed pattern in climate sensitivity ($p > 0.050$, CLASS-CTEM-N+, TEM6, VEGAS2.1), (Fig. 7 and Table S4).

3.3. Attribution of temperature effects to the effects of VPD and SMI

As previously reported, analysis of BAI data illustrated a strong negative relationship between temperature and growth during the previous summer, a signal that was underestimated by TBMs. We were interested in whether this negative relationship to temperature could be due to sensitivities related to modulations from drought-related covariates. We implemented partial GAMMs, where goodness-of-fit for models of BAI in relation to temperature was obtained whilst taking away the effects of vapour pressure deficit (VPD) and soil moisture index (SMI). After removing the effects of VPD and SMI, we found that most of the temperature signal was explained by VPD and SMI: only 7.6 % of the sites still had a significant relationship with summer and previous summer temperatures. SMI and VPD of the current year and the year prior to ring formation were significant determinants of BAI at 20 % of the sites. VPD was mostly negatively correlated to growth (60 % of the significant relationships) and SMI mostly positively correlated to growth (70 % of the significant relationships).

4. Discussion

The newly updated and spatially extensive national database of tree-ring measurements across Canada offered an unprecedented opportunity for benchmarking NPP simulations of TBMs with ground-based estimates of tree growth. Detecting commonalities between vegetation models and ground-based datasets enhances our confidence in how widely-used terrestrial biosphere models represent Canadian boreal/hemi-boreal forest sensitivity to climate variability. At the same time, identification of mismatches between datasets points out the ecological processes that might need revision

to reduce existing prediction uncertainties, highlighting promising avenues for future TBM development (Girardin et al., 2008; Zhang et al., 2018).

Our comparative analyses suggested that TBMs of the MsTMIP only partly reproduce the gradient of climate limitations on growth across the Canadian boreal/hemi-boreal zones. Specifically, patterns of growth sensitivity to climate obtained from analyses of tree-rings suggested that growth was largely determined by temperature in southwestern and eastern Canada (*i.e.,* in the Montane Cordillera and east of Boreal and Taiga Shields), and moisture availability in the northwest and south-central boreal zone (*i.e.,* in the Boreal Cordillera, Taiga Plains and Boreal Plains). VPD and SMI explained growth sensitivity to summer and previous summer temperature variability at most of the sites, suggesting that the dominant role of temperature on boreal tree growth was through VPD and SMI, which is consistent with previous studies (Price et al., 2013; Girardin et al., 2016a; Babst et al., 2019). We found an overall pattern of tree growth sensitivity to climate fluctuations, from water limitation in the northeast to thermal limitation in the southwest. This pattern was also inferred recently from a global meta-analysis of tree-ring data (Babst et al., 2019).

Our analysis indicated that the spatial patterns in NPP sensitivity to climate variation, particularly the southwest-northeast limiting gradient, were consistent with the pattern inferred from tree-ring data for a subset of the tested MsTMIP's TBMs, namely BIOME-BGC, DLEM, GTEC, ISAM, LPJ-wsl, SIB3-JPL, SIBCASA and ISAM. However, many of the TBMs underestimated the negative impact of increasing temperature and the positive impact of increasing precipitation on NPP (*e.g.,* BIOME-BGC, CLASS-CTEM-N+, DLEM, GTEC, VEGAS2.1, Figs. 6 and 7), as already found for boreal forests (Tei and Sugimoto, 2020). These biases brought significant deviations in the distribution of the climate sensitivity indices in these models (Fig. 7). This suggests those TBMs did not account for some of the detrimental temperature effects on growth, and failed to reproduce growth sensitivity to variability in seasonal precipitation. There are many possibilities for a negative relationship between growth and temperature. High temperatures decrease the amount of soil water available for growth first by increasing the vapour pressure deficit between leaf and air, which enhances evapotranspiration. When soil water supply is sufficient, increased temperature has a neutral to positive effect on growth, as in the northernmost environment, but after a certain threshold, temperature increase and the subsequent VPD increase can induce stomatal closure and reduced leaf conductance (Reich et al., 2018; López et al., 2021; Pau et al., 2022). Stomatal closure following increasing temperatures and drought conditions leads to a reduction in photosynthetic activity, generating carbon depletion, (Reich et al., 2018) and declines in tree growth and survival (Reich et al., 2022). Boreal tree species (such as *P. mariana* and *P. banksiana*) react to changes in the intensity and duration of droughts by adjusting stomatal conductance to maximise the trade-off between carbon gains and water losses (Marchand et al., 2021). TBMs simulate variations in canopy and leaf conductance in response to temperature and humidity variations, but the formulation of stomatal response and it's scaling up to canopy conductance do not necessarily reflect the latest studies on this topic (Medlyn et al., 2011; Reich et al., 2018). This is particularly true with respect to the response of stomatal conductance to temperature interactions with soil moisture or atmospheric carbon concentration, or with respect to how intrinsic species differences in stomatal sensitivity to water deficits regulate their sensitivity to climate warming (Reich et al., 2022). This deficiency was acknowledged as a reason for an oversensitivity of TBMs growth response to temperature variability and drought compared to assessments derived from by eddy-covariance data (Haxeltine and Prentice, 1996; Huntzinger et al., 2013; Zhang et al., 2018; Schwalm et al., 2019). Another point that may explain TBMs errors in estimation of forest growth sensitivity to temperature and precipitation variations, is the formulation of tree root system distribution, which has a strong influence on plant water uptake responses to climate variations (Arora and Boer, 2003; Girardin et al., 2008). TBMs often use a constant rooting depth, or a static rooting profile and do not account for the dynamic interplay between rooting patterns, resource availability, and resource uptake (Lu et al., 2019; Smithwick et al., 2014). Although different plant functional types and specific rooting parameterization are considered, this may not be sufficient to prevent either over- or under-estimation of root resource uptake (Drewniak, 2019). Ongoing developments that integrate direct soil water-growth response functions and model direct environmental control of plant growth may improve TBM estimate of NPP (Friend et al., 2019; Eckes-Shephard et al., 2021).

Another possible reason for why TBMs overestimated temperature effects might be because dark respiration in these models is not well formulated. In addition to their effects on water availability, high temperature can also hamper tree growth by affecting dark respiration rates, as demonstrated for some species such as *Picea mariana,* even if some degree of thermal acclimation occurs over time (Girardin et al., 2016a; Reich et al., 2016; Grossiord et al., 2020). Where increases in dark respiration are not compensated for by increases in photosynthesis (for example if water availability is low), growth may be suppressed, particularly at warm locations where the probability of growth dependence on respiration is high (Girardin et al., 2016a; Dusenge et al., 2021). TBMs that do not formulate dark respiration changes following temperature variability might underestimate the negative temperature impact on net productivity and biomass growth (Lu et al., 2020).

The comparisons of growth data obtained from tree rings and from TBMs also provided indications that TBMs tend to overestimate the importance of winter-spring temperature in driving NPP. One plausible explanation for this may be that TBMs of the MsTMIP underestimate water limitation in some regions, where the benefit of above average spring temperatures on productivity is cancelled out by significant drought stress. This stress can occur during spring or during the subsequent summer, either due to continued increasing temperatures or to the depletion of water resources during spring growth (Wang et al., 2011; Buermann et al., 2018; Lian et al., 2020). Alternatively, an inaccurate formulation of leaf phenology and/or of the phenology of light use efficiency, with leaves being mature in summer and benefiting more from higher radiation and temperature in summer than in spring, may explain why the influence of spring temperature is overestimated in TBMs (Montgomery et al., 2020). The photoperiod and temperature at the end of spring are more important determinants of a plant's productivity than the growing season length, as they allow optimal photosynthesis when light use efficiency peaks following leaf maturation (Keenan et al., 2014; Park et al., 2019).

Growth sensitivity to climate based on tree-ring series was highly sensitive to temperature and precipitation of the summer prior to ring formation, suggesting "carry-over" effects of the previous year's climate on tree growth (Wettstein et al., 2011). This may result from the storage of non-structural carbohydrates (NSCs) allocated to growth according to climate and nutrient availability (Richardson et al., 2013; Teets et al., 2018; Pappas et al., 2020). For example, carbon storage pools of *Populus* trees recover after a drought, from the crown to the roots, creating a time lag in growth response to climate (Fatichi et al., 2019). Such dynamic allocation of non-structural carbohydrates can be integrated in TBMs by using simulation time steps longer than assimilation lag times (Girardin et al., 2016a; Teets et al., 2018; Schiestl-Aalto et al., 2019; Huang et al., 2021; also see Fig. S3), or by integrating carbon assimilation lags through allocation to multiple and separate carbon pools (Richardson et al., 2013; Pappas et al., 2020). Eight of the TBMs we tested (Biome-BGC, CLASS-CTEM-N+, CLM4, CLM4-VIC, LPJ-wsl, ORCHIDEE-LSCE, SIBCASA, and VISIT) integrate the modelling of a carbohydrate reserve biomass pool (Huntzinger et al., 2013). For the five TBMs where aboveground biomass outputs were made available, those with a carbon reserve pool to some extent lagged the response to climate variations (see Fig. 6). Omitting a carbon reserve pool in TBMs has already been highlighted as a shortcoming of TBMs implemented in temperate forests (Babst et al., 2014a). Kolus et al. (2019) also found weaker growth sensitivity to drought in simulations compared to observed growth. Understanding how non-structural carbohydrates influence growth, as well as other mechanisms driving lagged effects on growth, remains an active area of research (Cabon et al., 2022). Major developments, like using oxygen and carbon isotopes to trace

carbon assimilation and allocation to wood production, will likely enlighten future formulation of the physiological processes driving growth in TBMs (Friend et al., 2019; Barichivich et al., 2021).

Growth sensitivity to climate variability for the five major tree species we examined were heterogeneous across Canada, and consistent with previous observations for *Picea mariana* and *Pinus banksiana* (Marchand et al., 2021). While $Climate_{Index}$ patterns of *Picea glauca* and *Populus tremuloides* species were very similar to the overall $Climate_{Index}$ pattern, *Pinus contorta* displayed a different $Climate_{Index}$ pattern: high temperature sensitivity in the south-western Boreal Shield and south-eastern Boreal Cordillera (Figs. 1 and 3). These species-specific differences in $Climate_{Index}$ pattern are likely due to differential responses to climate variability among species and ecotypes (Haxeltine and Prentice, 1996; Reich et al., 2014; Reich and Oleksyn, 2008), and how these responses vary geographically within each species, which is likely important but poorly quantified. Several plant functional types (PFT) are considered and parameterized in TBMs, but boreal/hemi-boreal forests are not represented by more than three plants functional types, and no TBMs explicitly include ecotypic variation, although this was explored in Reich et al. (2014). Species-specific heterogeneity in sensitivity to climate variations observed among the monospecific sites data suggests that accounting for differences in flora composition among sites is a key aspect of TBM performance that could be improved (Breitenmoser et al., 2014). We recognize these suggestions for improvement will not resolve all of the different model uncertainties, including those inherent to disturbance history, soil properties (drainage, texture), and anthropogenic pressure. Eventually, other types of models with a tree-based approach, like StandLEAP (Girardin et al., 2016a) or MAIDEN (Gennaretti et al., 2017), might provide better simulations of tree ecophysiological responses to climate and perspectives for subsequent terrestrial biosphere model development. These two tree-based approaches to modelling growth have shown good performance in comparisons of simulation results with CO_2 flux measurements by tower-based eddy-covariance systems and with tree-ring data over Canada.

5. Conclusion

Our analysis of a large temporal and spatial scale tree-ring dataset provides insight into Canadian boreal and hemi-boreal forest growth sensitivities to interannual temperature and precipitation variations. We confirmed a southwest to northeast pattern in growth sensitivity related to a gradient of decreasing water to increasing thermal limitation (Babst et al., 2019). Our analyses also highlighted lagged growth sensitivities to annual temperature variability, with growth largely determined by the climate during the summer prior to ring formation. Because the best performing TBMs should reproduce the observed spatial gradient in climate limitations, and the mean of their distribution, we can determine that these models are performing reasonably best: CLM4, CLM4-VIC, ISAM, LPJ-wsl and VISIT. Of those, CLM4, CLM4-VIC, LPJ-wsl and VISIT integrate a carbon reserve pool. However, TBMs generally failed to reproduce sensitivities to previous summer temperature and precipitation, and current-year spring temperature. Our results illustrate a mechanistic weakness of some of TBMs where the growth of plant biomass is simulated directly from leaf photosynthesis, without considering the process of wood formation. Adding the missing processes of wood formation (Zuidema et al., 2018), and integrating the latest developments in the formulation of within and among species differences in leaf conductance, leaf longevity, rooting dynamics and depth, and carbon storage dynamics, improve projections of forest productivity for boreal and hemi-boreal forests of Canada (Bonan, 2019; Friend et al., 2019; Reich et al., 2014; Zuidema et al., 2018). In those respects, observed tree-ring data as used here would be of primary importance to calibrate and validate new model developments, as already initiated in some models using Bayesian optimization to estimate model parameters from observed dynamics (Gennaretti et al., 2017; Rezsöhazy et al., 2020; Evans et al., 2022).

CRediT authorship contribution statement

M.P.G, D.W., and A.M. conceived this work, A.M. and M.P.G. wrote the original manuscript. All authors discussed and interpreted the results and contributed to the manuscript.

Data availability

Data will be made available on request.

Declaration of competing interest

The authors declare that they have no known competing financial interests or personal relationships that could have appeared to influence the work reported in this paper.

Acknowledgement

We thank Deborah Huntzinger, Associate Professor at School of Earth and Sustainability from Northern Arizona University for proof reading on an earlier version of the manuscript.

Funding

This research was funded by a Strategic and Discovery Grant of the Natural Sciences and Engineering Research Council of Canada (D. Way, M.P. Girardin) and Canadian Forest Service funds (M.P. Girardin, E. M. Campbell, J. Metsaranta, A. Arseneault). D. Way is also partially supported through the United States Department of Energy contract no. DE-SC0012704 to Brookhaven National Laboratory. P. Reich is supported by the U.S. National Science Foundation Biological Integration Institutes Grant NSF-DBI-2021898.We would like to thank all the people, as well as the funding agencies, who contributed to the development and applications of the different models and data used in this work.

Data availability

Tree-ring datasets assembled during this study have been deposited in the TreeSource repository, https://treesource.rncan.gc.ca/en. Restrictions may apply to the availability of third-party raw data (*e.g.*, Canada's NFI, ABMI, MFFPQ), which were used under agreements, and so are not yet publicly available. Reasonable requests for accessing such data can be made to authors and with permission of the data contributors (contact names are included in the TreeSource repository). Annual NPP simulations were retrieved from the MsTMIP v1 ensemble of terrestrial biosphere model simulations generated by the North American Carbon Program (NACP, https://daac.ornl.gov/cgi-bin/dsviewer.pl?ds_id=1225). Weather data are freely accessible through Environment Canada's portal (https://climate.weather.gc.ca/) and the BioSIM server (https://cfs.nrcan.gc.ca/projects/133).

Code availability

No custom code or mathematical algorithms were used in the analyses of these data. The R code for our statistical analyses is available from the authors upon request, and each of the R packages used is referenced in the Methods.

Appendix A. Supplementary data

Supplementary data to this article can be found online at https://doi.org/10.1016/j.scitotenv.2022.158062.

References

Arora, V.K., Boer, G.J., 2003. A representation of variable root distribution in dynamic vegetation models. Earth Interact. 7 (6), 1–19.

Babst, F., Bouriaud, O., Alexander, R., Trouet, V., Frank, D., 2014a. Toward consistent measurements of carbon accumulation: a multi-site assessment of biomass and basal area increment across Europe. Dendrochronologia 32 (2), 153–161.

Babst, F., Bouriaud, O., Papale, D., Gielen, B., Janssens, I.A., Nikinmaa, E., Ibrom, A., Wu, J., Bernhofer, C., Köstner, B., et al., 2014b. Above-ground woody carbon sequestration measured from tree rings is coherent with net ecosystem productivity at five eddy-covariance sites. New Phytol. 201 (4), 1289–1303.

Babst, F., Bodesheim, P., Charney, N., Friend, A.D., Girardin, M.P., Klesse, S., Moore, D.J.P., Seftigen, K., Björklund, J., Bouriaud, O., et al., 2018. When tree rings go global: challenges and opportunities for retro-and prospective insight. Quat. Sci. Rev. 197, 1–20.

Babst, F., Bouriaud, O., Poulter, B., Trouet, V., Girardin, M.P., Frank, D.C., 2019. Twentieth century redistribution in climatic drivers of global tree growth. ScienceAdvances 5 (1), eaat4313.

Barichivich, J., Peylin, P., Launois, T., Daux, V., Risi, C., Jeong, J., Luyssaert, S., 2021. A triple tree-ring constraint for tree growth and physiology in a global land surface model. Biogeosciences 18 (12), 3781–3803.

Barton, K., Barton, M.K., 2015. Package 'mumin'. Version 1 (18), 439.

Blyth, E.M., Arora, V.K., Clark, D.B., Dadson, S.J., de Kauwe, M.G., Lawrence, D.M., Melton, J.R., Pongratz, J., Turton, R.H., Yoshimura, K., et al., 2021. Advances in land surface modelling. Curr. Clim. Chang. Rep. 7 (2), 45–71.

Bonan, G., 2019. Stomatal conductance. Climate Change and Terrestrial Ecosystem Modeling. Cambridge University Press, pp. 189–212.

Brandt, J.P., Flannigan, M.D., Maynard, D.G., Thompson, I.D., Volney, W.J.A., 2013. An introduction to Canada's boreal zone: ecosystem processes, health, sustainability, and environmental issues. Environ. Rev. 21 (4), 207–226.

Breitenmoser, P., Brönnimann, S., Frank, D., 2014. Forward modelling of tree-ring width and comparison with a global network of tree-ring chronologies. Clim. Past 10 (2), 437–449.

Buermann, W., Forkel, M., O'sullivan, M., Sitch, S., Friedlingstein, P., Haverd, V., Jain, A.K., Kato, E., Kautz, M., Lienert, S., et al., 2018. Widespread seasonal compensation effects of spring warming on northern plant productivity. Nature 562 (7725), 110–114.

Burnham, K.P., Anderson, D.R., 2002. A practical information-theoretic approach. Model Selection and Multimodel Inference. 2, pp. 70–71.

Cabon, A., Kannenberg, S.A., Arain, A., Babst, F., Baldocchi, D., Belmecheri, S., Delpierre, N., Guerrieri, R., Maxwell, J.T., McKenzie, S., et al., 2022. Cross-biome synthesis of source versus sink limits to tree growth. Science 376 (6594), 758–761.

Drewniak, B.A., 2019. Simulating dynamic roots in the energy exascale earth system land model. J. Adv. Mode. Earth Syst. 11 (1), 338–359.

Dusenge, M.E., Ward, E.J., Warren, J.M., Stinziano, J.R., Wullschleger, S.D., Hanson, P.J., Way, D.A., 2021. Warming induces divergent stomatal dynamics in co-occurring boreal trees. Glob. Chang. Biol. 27 (13), 3079–3094.

Dutilleul, P., Clifford, P., Richardson, S., Hemon, D., 1993. Modifying the t test for assessing the correlation between two spatial processes. Biometrics 305–314.

Eckes-Shephard, A.H., Tiavlovsky, E., Chen, Y., Fonti, P., Friend, A.D., 2021. Direct response of tree growth to soil water and its implications for terrestrial carbon cycle modelling. Glob. Chang. Biol. 27 (1), 121–135.

Ecological Stratification Working Group, 2016. A national ecological framework for Canada. Agriculture and Agri-Food Canada, Research Branch, Centre for Land and Biological Resources Research, and Environment Canada, State of the Environment Directorate, Ecozone Analysis Branch, Ottawa/Hull. Report and National Map at 1:7,500,000 scale.

ESRI, 2011. ArcGIS Desktop Release 10. 437. Environmental Systems Research Institute, Redlands, CA, p. 438.

Evans, M.E.K., DeRose, R.J., Klesse, S., Girardin, M.P., Heilman, K.A., Alexander, M.R., Arsenault, A., Babst, F., Bouchard, M., Cahoon, S.M.P., Campbell, E.M., Dietze, M., Duchesne, L., Frank, D.C., Giebink, C.L., G´omez-Guerrero, A., García, G.G., Hogg, E.H., Metsaranta, J., Ols, C., Rayback, S.A., Reid, A., Ricker, M., Schaberg, P.G., Shaw, J.D., Sullivan, P.F., Gayt´an, S.A.V., 2022. Adding tree rings to North America's national forest inventories: an essential tool to guide drawdown of atmospheric CO2. Bioscience 72 (3), 233–246.

Fatichi, S., Pappas, C., Zscheischler, J., Leuzinger, S., 2019. Modelling carbon sources and sinks in terrestrial vegetation. New Phytol. 221 (2), 652–668.

Fisher, J.B., Sikka, M., Block, G.L., Schwalm, C.R., Parazoo, N.C., Kolus, H.R., Sok, M., Wang, A., Gagne-Landmann, A., Lawal, S., et al., 2022. The terrestrial biosphere model farm. J. Adv. Model. Earth Syst. 14 (2), e2021MS002676.

Friend, A.D., Eckes-Shephard, A.H., Fonti, P., Rademacher, T.T., Rathgeber, C.B.K., Richardson, A.D., Turton, R.H., 2019. On the need to consider wood formation processes in global vegetation models and a suggested approach. Ann. For. Sci. 76 (2), 1–13.

Gauthier, S., Bernier, P., Burton, P.J., Edwards, J., Isaac, K., Isabel, N., Jayen, K., le Goff, H., Nelson, E.A., 2014. Climate change vulnerability and adaptation in the managed Canadian boreal forest. Environ. Rev. 22 (3), 256–285.

Gennaretti, F., Gea-Izquierdo, G., Boucher, E., Berninger, F., Arseneault, D., Guiot, J., 2017. Ecophysiological modeling of photosynthesis and carbon allocation to the tree stem in the boreal forest. Biogeosciences 14 (21), 4851–4866.

Gillis, M.D., Omule, A.Y., Brierley, T., 2005. Monitoring Canada's forests: the national forest inventory. For. Chron. 81 (2), 214–221.

Girardin, M.P., Raulier, F., Bernier, P.Y., Tardif, J.C., 2008. Response of tree growth to a changing climate in boreal Central Canada: a comparison of empirical, process-based, and hybrid modelling approaches. Ecol. Model. 213 (2), 209–228.

Girardin, M.P., Guo, X.J., de Jong, R., Kinnard, C., Bernier, P., Raulier, F., 2014. Unusual forest growth decline in boreal North America covaries with the retreat of Arctic Sea ice. Glob. Chang. Biol. 20 (3), 851–866.

Girardin, M.P., Hogg, E.H., Bernier, P.Y., Kurz, W.A., Guo, X.J., Cyr, G., 2016a. Negative impacts of high temperatures on growth of black spruce forests intensify with the anticipated climate warming. Glob. Chang. Biol. 22 (2), 627–643.

Girardin, M.P., Bouriaud, O., Hogg, E.H., Kurz, W., Zimmermann, N.E., Metsaranta, J.M., de Jong, R., Frank, D.C., Esper, J., Büntgen, U., et al., 2016b. No growth stimulation of Canada's boreal forest under half-century of combined warming and CO2 fertilization. Proc. Natl. Acad. Sci. 113 (52), E8406–E8414.

Girardin, M.P., Guo, X.J., Metsaranta, J., Gervais, D., Campbell, E., Arsenault, A., Isaac-Renton, M., Harvey, J.E., Bhatti, J., Hogg, E.H., 2021. A national tree-ring data repository for Canadian forests (CFS-TRenD): structure, synthesis, and applications. Environ. Rev. 29 (2), 225–241.

Grossiord, C., Buckley, T.N., Cernusak, L.A., Novick, K.A., Poulter, B., Siegwolf, R.T.W., Sperry, J.S., McDowell, N.G., 2020. Plant responses to rising vapor pressure deficit. New Phytol. 226 (6), 1550–1566.

Haxeltine, A., Prentice, I.C., 1996. BIOME3: an equilibrium terrestrial biosphere model based on ecophysiological constraints, resource availability, and competition among plant functional types. Glob. Biogeochem. Cycl. 10 (4), 693–709.

Hogg, E.H., Brandt, J.P., Kochtubajda, B., 2005. Factors affecting interannual variation in growth of western Canadian aspen forests during 1951–2000. Can. J. For. Res. 35 (3), 610–622.

Hogg, E.H., Barr, A.G., Black, T.A., 2013. A simple soil moisture index for representing multi-year drought impacts on aspen productivity in the western Canadian interior. Agric. For. Meteorol. 178, 173–182.

Huang, J., Hammerbacher, A., Gershenzon, J., van Dam, N.M., Sala, A., McDowell, N.G., Chowdhury, S., Gleixner, G., Trumbore, S., Hartmann, H., 2021. Storage of carbon reserves in spruce trees is prioritized over growth in the face of carbon limitation. Proc. Natl. Acad. Sci. 118 (33).

Huntzinger, D.N., Schwalm, C., Michalak, A.M., Schaefer, K., King, A.W., Wei, Y., Jacobson, A., Liu, S., Cook, R.B., Post, W.M., et al., 2013. The north american carbon program multi-scale synthesis and terrestrial model intercomparison project–part 1: overview and experimental design. Geosci. Model Dev. 6 (6), 2121–2133.

Keenan, T.F., Gray, J., Friedl, M.A., Toomey, M., Bohrer, G., Hollinger, D.Y., Munger, J.W., O'Keefe, J., Schmid, H.P., Wing, I.S., et al., 2014. Net carbon uptake has increased through warming-induced changes in temperate forest phenology. Nat. Clim. Chang. 4 (7), 598–604.

King, D.A., Turner, D.P., Ritts, W.D., 2011. Parameterization of a diagnostic carbon cycle model for continental scale application. Remote Sens. Environ. 115 (7), 1653–1664.

Klesse, S., Babst, F., Lienert, S., Spahni, R., Joos, F., Bouriaud, O., Carrer, M., di Filippo, A., Poulter, B., Trotsiuk, V., et al., 2018. A combined tree ring and vegetation model assessment of European forest growth sensitivity to interannual climate variability. Glob. Biogeochem. Cycles 32 (8), 1226–1240.

Kolus, H.R., Huntzinger, D.N., Schwalm, C.R., Fisher, J.B., McKay, N., Fang, Y., Michalak, A.M., Schaefer, K., Wei, Y., Poulter, B., et al., 2019. Land carbon models underestimate the severity and duration of drought's impact on plant productivity. Sci. Rep. 9 (1), 1–10.

Lagergren, F., Jönsson, A.M., Linderson, H., Lindroth, A., 2019. Time shift between net and gross CO2 uptake and growth derived from tree rings in pine and spruce. Trees 33 (3), 765–776.

Lavoie, J., Montoro Girona, M., Morin, H., 2019. Vulnerability of conifer regeneration to spruce budworm outbreaks in the eastern Canadian boreal forest. Forests 10 (10), 850.

Létourneau, J.P., Matejek, S., Morneau, C., Robitaille, A., Roméo, T., Brunelle, J., Leboeuf, A., 2008. Norme de cartographie écoforestière du Programme d'inventaire écoforestier nordique. Ministère Des Ressources Naturelles et de La Faune Du Québec, Québec, QC.

Lian, X., Piao, S., Li, L.Z.X., Li, Y., Huntingford, C., Ciais, P., Cescatti, A., Janssens, I.A., Peñuelas, J., Buermann, W., et al., 2020. Summer soil drying exacerbated by earlier spring greening of northern vegetation. ScienceAdvances 6 (1), eaax0255.

Loader, N.J., McCarroll, D., Gagen, M., Robertson, I., Jalkanen, R., 2007. Extracting climatic information from stable isotopes in tree rings. Terrestrial Ecol. 1, 25–48.

López, J., Way, D.A., Sadok, W., 2021. Systemic effects of rising atmospheric vapor pressure deficit on plant physiology and productivity. Glob. Chang. Biol. 27 (9), 1704–1720.

Lu, H., Yuan, W., Chen, X., 2019. A processes-based dynamic root growth model integrated into the ecosystem model. J. Adv. Model. Earth Syst. 11 (12), 4614–4628.

Lu, X., Ju, W., Li, J., Croft, H., Chen, J.M., Luo, Y., Yu, H., Hu, H., 2020. Maximum carboxylation rate estimation with chlorophyll content as a proxy of rubisco content. J. Geophys. Res. Biogeosci. 125 (8), e2020JG005748.

Marchand, W., Girardin, M.P., Hartmann, H., Lévesque, M., Gauthier, S., Bergeron, Y., 2021. Contrasting life-history traits of black spruce and jack pine influence their physiological response to drought and growth recovery in northeastern boreal Canada. Sci. Total Environ. 794, 148514.

Medlyn, B.E., Duursma, R.A., Eamus, D., Ellsworth, D.S., Prentice, I.C., Barton, C.V.M., Crous, K.Y., de Angelis, P., Freeman, M., Wingate, L., 2011. Reconciling the optimal and empirical approaches to modelling stomatal conductance. Glob. Chang. Biol. 17 (6), 2134–2144.

Medlyn, B.E., Zaehle, S., de Kauwe, M.G., Walker, A.P., Dietze, M.C., Hanson, P.J., Hickler, T., Jain, A.K., Luo, Y., Parton, W., et al., 2015. Using ecosystem experiments to improve vegetation models. Nat. Clim. Chang. 5 (6), 528–534.

Metsaranta, J.M., Trofymow, J.A., Black, T.A., Jassal, R.S., 2018. Long-term time series of annual ecosystem production (1985–2010) derived from tree rings in Douglas-fir stands on Vancouver Island, Canada using a hybrid biometric-modelling approach. For. Ecol. Manag. 429, 57–68.

Metsaranta, J.M., Mamet, S.D., Maillet, J., Barr, A.G., 2021. Comparison of tree-ring and eddy-covariance derived annual ecosystem production estimates for jack pine and trembling aspen forests in Saskatchewan, Canada. Agric. For. Meteorol. 307, 108469.

Montgomery, R.A., Rice, K.E., Stefanski, A., Rich, R.L., Reich, P.B., 2020. Phenological responses of temperate and boreal trees to warming depend on ambient spring temperatures, leaf habit, and geographic range. Proc. Natl. Acad. Sci. 117 (19), 10397–10405.

Ols, C., Girardin, M.P., Hofgaard, A., Bergeron, Y., Drobyshev, I., 2018. Monitoring climate sensitivity shifts in tree-rings of eastern boreal North America using model-data comparison. Ecosystems 21 (5), 1042–1057.

Pan, Y., Birdsey, R.A., Fang, J., Houghton, R., Kauppi, P.E., Kurz, W.A., Phillips, O.L., Shvidenko, A., Lewis, S.L., Canadell, J.G., et al., 2011. A large and persistent carbon sink in the world's forests. Science 333 (6045), 988–993.

Pappas, C., Maillet, J., Rakowski, S., Baltzer, J.L., Barr, A.G., Black, T.A., Fatichi, S., Laroque, C.P., Matheny, A.M., Roy, A., et al., 2020. Aboveground tree growth is a minor and decoupled fraction of boreal forest carbon input. Agric. For. Meteorol. 290, 108030.

Park, T., Chen, C., Macias-Fauria, M., Tømmervik, H., Choi, S., Winkler, A., Bhatt, U.S., Walker, D.A., Piao, S., Brovkin, V., et al., 2019. Changes in timing of seasonal peak photosynthetic activity in northern ecosystems. Glob. Chang. Biol. 25 (7), 2382–2395.

Pau, M., Gauthier, S., Chavardès, R.D., Girardin, M.P., Marchand, W., Bergeron, Y., 2022. Site index as a predictor of the effect of climate warming on boreal tree growth. Glob. Chang. Biol. 28 (5), 1903–1918.

Price, D.T., Alfaro, R.I., Brown, K.J., Flannigan, M.D., Fleming, R.A., Hogg, E.H., Girardin, M.P., Lakusta, T., Johnston, M., McKenney, D.W., et al., 2013. Anticipating the consequences of climate change for Canada's boreal forest ecosystems. Environ. Rev. 21 (4), 322–365.

Régnière, J., Bolstad, P., 1994. Statistical simulation of daily air temperature patterns eastern North America to forecast seasonal events in insect pest management. Environ. Entomol. 23 (6), 1368–1380.

Régnière, J., Saint-Amant, R., Béchard, A., Moutaoufik, A., 2014. BioSIM 10: User's Manual. Laurentian Forestry Centre.

Reich, P.B., Oleksyn, J., 2008. Climate warming will reduce growth and survival of Scots pine except in the far north. Ecol. Lett. 11 (6), 588–597.

Reich, P.B., Rich, R.L., Lu, X., Wang, Y.-P., Oleksyn, J., 2014. Biogeographic variation in evergreen conifer needle longevity and impacts on boreal forest carbon cycle projections. Proc. Natl. Acad. Sci. 111 (38), 13703–13708.

Reich, P.B., Sendall, K.M., Stefanski, A., Wei, X., Rich, R.L., Montgomery, R.A., 2016. Boreal and temperate trees show strong acclimation of respiration to warming. Nature 531 (7596), 633–636.

Reich, P.B., Sendall, K.M., Stefanski, A., Rich, R.L., Hobbie, S.E., Montgomery, R.A., 2018. Effects of climate warming on photosynthesis in boreal tree species depend on soil moisture. Nature 562 (7726), 263–267.

Reich, P.B., Bermudez, R., Montgomery, R.A., Rich, R.L., Rice, K.E., Hobbie, S.E., Stefanski, A., 2022. Even modest climate change may lead to major transitions in boreal forests. Nature 608, 540–545. https://doi.org/10.1038/s41586-022-05076-3.

Rezsöhazy, J., Goosse, H., Guiot, J., Gennaretti, F., Boucher, E., André, F., Jonard, M., 2020. Application and evaluation of the dendroclimatic process-based model MAIDEN during the last century in Canada and Europe. Clim. Past 16 (3), 1043–1059.

Richardson, A.D., Carbone, M.S., Keenan, T.F., Czimczik, C.I., Hollinger, D.Y., Murakami, P., Schaberg, P.G., Xu, X., 2013. Seasonal dynamics and age of stemwood nonstructural carbohydrates in temperate forest trees. New Phytol. 197 (3), 850–861.

Rossi, S., Morin, H., Deslauriers, A., 2012. Causes and correlations in cambium phenology: towards an integrated framework of xylogenesis. J. Exp. Bot. 63 (5), 2117–2126.

Sánchez-Pinillos, M., Leduc, A., Ameztegui, A., Kneeshaw, D., Lloret, F., Coll, L., 2019. Resistance, resilience or change: post-disturbance dynamics of boreal forests after insect outbreaks. Ecosystems 22 (8), 1886–1901.

Schiestl-Aalto, P., Ryhti, K., Mäkelä, A., Peltoniemi, M., Bäck, J., Kulmala, L., 2019. Analysis of the NSC storage dynamics in tree organs reveals the allocation to belowground symbionts in the framework of whole tree carbon balance. Front. Forests Glob. Chang. 2, 17.

Schwalm, C.R., Schaefer, K., Fisher, J.B., Huntzinger, D., Elshorbany, Y., Fang, Y., Hayes, D., Jafarov, E., Michalak, A.M., Piper, M., et al., 2019. Divergence in land surface modeling: linking spread to structure. Environ. Res. Commun. 1 (11), 111004.

Serreze, M.C., Walsh, J.E., Chapin, F.S., Osterkamp, T., Dyurgerov, M., Romanovsky, V., Oechel, W.C., Morison, J., Zhang, T., Barry, R.G., 2000. Observational evidence of recent change in the northern high-latitude environment. Clim. Chang. 46 (1), 159–207.

Smithwick, E.A.H., Lucash, M.S., McCormack, M.L., Sivandran, G., 2014. Improving the representation of roots in terrestrial models. Ecol. Model. 291, 193–204.

Spawn, S.A., Gibbs, H.K., 2020. Global Aboveground and Belowground Biomass Carbon Density Maps for the Year 2010. ORNL DAAC.

Teets, A., Fraver, S., Hollinger, D.Y., Weiskittel, A.R., Seymour, R.S., Richardson, A.D., 2018. Linking annual tree growth with eddy-flux measures of net ecosystem productivity across twenty years of observation in a mixed conifer forest. Agric. For. Meteorol. 249, 479–487.

Tei, S., Sugimoto, A., 2020. Excessive positive response of model-simulated land net primary production to climate changes over circumboreal forests. Plant-Environ. Interact. 1 (2), 102–121.

Trenberth, K.E., 1983. What are the seasons? Bull. Am. Meteorol. Soc. 64 (11), 1276–1282.

Vallejos, R., Osorio, F., Bevilacqua, M., 2020. Spatial Relationships Between Two Georeferenced Variables: With Applications in R. Springer Nature.

Wang, X., Piao, S., Ciais, P., Li, J., Friedlingstein, P., Koven, C., Chen, A., 2011. Spring temperature change and its implication in the change of vegetation growth in North America from 1982 to 2006. Proc. Natl. Acad. Sci. 108 (4), 1240–1245.

Wang, J.A., Baccini, A., Farina, M., Randerson, J.T., Friedl, M.A., 2021. Disturbance suppresses the aboveground carbon sink in north american boreal forests. Nat. Clim. Chang. 11 (5), 435–441.

Wei, Y., Liu, S., Huntzinger, D.N., Michalak, A.M., Viovy, N., Post, W.M., Schwalm, C.R., Schaefer, K., Jacobson, A.R., Lu, C., et al., 2014. The north american carbon program multi-scale synthesis and terrestrial model intercomparison project–part 2: environmental driver data. Geosci. Model Dev. 7 (6), 2875–2893.

Wettstein, J.J., Littell, J.S., Wallace, J.M., Gedalof, Z., 2011. Coherent region-, species-, and frequency-dependent local climate signals in northern hemisphere tree-ring widths. J. Clim. 24 (23), 5998–6012.

Wood, S.N., 2006. Generalized Additive Models: An Introduction With R.

Wulder, M.A., Hermosilla, T., White, J.C., Coops, N.C., 2020. Biomass status and dynamics over Canada's forests: disentangling disturbed area from associated aboveground biomass consequences. Environ. Res. Lett. 15 (9), 94093.

Zhang, Z., Babst, F., Bellassen, V., Frank, D., Launois, T., Tan, K., Ciais, P., Poulter, B., 2018. Converging climate sensitivities of european forests between observed radial tree growth and vegetation models. Ecosystems 21 (3), 410–425.

Zscheischler, J., Michalak, A.M., Schwalm, C., Mahecha, M.D., Huntzinger, D.N., Reichstein, M., Berthier, G., Ciais, P., Cook, R.B., El-Masri, B., et al., 2014. Impact of large-scale climate extremes on biospheric carbon fluxes: an intercomparison based on MsTMIP data. Glob. Biogeochem. Cycl. 28 (6), 585–600.

Zuidema, P.A., Poulter, B., Frank, D.C., 2018. A wood biology agenda to support global vegetation modelling. Trends Plant Sci. 23 (11), 1006–1015.